

Response to Referee #1

We greatly appreciate the time and effort that referee 1 spent in reviewing our manuscript. Below we make a point-by-point response to these comments. According to editor's requirement, the response to the referee 1 is structured in the following sequence: (1) comments from the referee in black color, (2) our response in blue color, and (3) our changes in the revised manuscript in red color.

Although I find the authors' explanations reasonable, I feel that they should add a sentence or two in the manuscript to clarify:

1. why they decide to use a PILS

10

Taking the referee's suggestion, we have added two sentences in the third paragraph in Sec. 2.2 in the revised manuscript.

The PILS samples water-soluble species in particles. As the SOA compositions are almost all water-soluble species, it is reasonable and reliable to use PILS to sample SOA for analysis of chemical composition.

15

2. that the HPLC was only used as an injection system

Taking the referee's suggestion, we have added a sentence in last paragraph in Sec. 2.2 in the revised manuscript.

20 In this study, the UPLC was only used as the injection system of HRMS.

Response to Referee #3

We greatly appreciate the time and effort that referee 3 spent in reviewing our manuscript. The comments are really thoughtful and helpful to improve the quality of our paper. Referee 3 has provided both main comments and other specific comments. Below we make a point-by-point response to these comments. According to editor's requirement, the response to the referee 3 is structured in the following sequence: (1) comments from the referee in black color, (2) our response in blue color, and (3) our changes in the revised manuscript in red color.

The study proposed by Zhang et al, presents new results related to the effect of relative humidity on the formation and composition of SOA generated from the OH-initiated oxidation of xylene. While it is an interesting topic, this study cannot be published as it is, as different aspects/conclusions of the paper are not well constrained or speculative (see below). I suggest that the authors have a close look at the existing literature and provide strong(er) evidence (e.g., MS2 spectra, ...) to support their statements.

1. Page 2, lines 33-34: Please provide references and/or results.

In fact, the references have been given at the end of the mentioned sentence (Jia and Xu, 2014, 2018) in the revised manuscript. Taking the referee's suggestion, we have added two sentences about the results following the mentioned sentence in the revised manuscript.

In these studies, O-H, C=O, C-O, and C-OH were found to be the main functional groups, intensities of which largely increased with increasing RH. Compounds in SOA with the O-H group mainly contributed to the increasement of SOA, such as polyalcohols formed from aqueous reactions.

2. Page 3. Lines 4-15. This section is not useful/needed, especially as it is disconnected to the rest of the introduction. The authors mainly focused on particle phase processes. Different aspects are actually missing including acidity effect (directly linked to LWC) and/or viscosity/phase effect on particle-phase reactions and can be added to the introduction.

Taking the referee's suggestion, we have deleted this section in the revised manuscript. We have also added several sentences about the acidity effect and viscosity/phase effect on particle-phase reaction at the end of the third paragraph in the introduction section in the revised manuscript.

Acid-catalysis of heterogeneous reactions of atmospheric organic carbonyl species in particle phase can lead to a large increase of SOA mass, while this process can be suppressed by the lower acidity at high RH (Czochke et al., 2003). In

addition, RH can change the viscosity of SOA and further affect the chemical processes of SOA formation (Kidd et al., 2014; Liu et al., 2017).

Czoschke, N. M., Jang, M., and Kamens, R. M.: Effect of acidic seed on biogenic secondary organic aerosol growth, *Atmos. Environ.*, **37**, 4287-4299, 10.1016/s1352-2310(03)00511-9, 2003.

Kidd, C., Perraud, V., Wingen, L. M., and Finlayson-Pitts, B. J.: Integrating phase and composition of secondary organic aerosol from the ozonolysis of alpha-pinene, *Proc. Natl. Acad. Sci. U. S. A.*, **111**, 7552-7557, 10.1073/pnas.1322558111, 2014.

Liu, Y., Wu, Z., and Hu, M.: Advances in the phase state of secondary organic aerosol (in Chinese), *China Environ. Sci.*, **37**, 1637-1645, 2017.

3. Paragraph 3.1. This section should be revised and better organized. As it is, it is very difficult to follow. In addition, the authors should discuss the impact of reacted VOC on SOA yields when comparing different studies.

15 Taking the referee's advice, we have revised and reorganized the Sec. 3.1 for the clear understanding. The referee 4 suggested us to add some experiments at different RHs, of which results have been included in the revised Sec. 3.1. The impact of reacted *m*-xylene on SOA yields has been also included in the revised manuscript based on the newly added Fig. 2 according to the comment 7.

20 Seven experiments were conducted. The initial conditions, the LWC, SOA concentrations, yields and reacted *m*-xylene at the end of each experiment in *m*-xylene-H₂O₂ photooxidation system are summarized in Table 1. Exps. 1 and 2 were conducted in dry zero air, which are defined as the low RH experiments. Exps. 6 and 7 were conducted in humid zero air, which are defined as the high RH experiments. Exps. 3-5 were conducted in the mixed air of dry and humid zero air, which are defined as the intermediate RH experiments. Under intermediate and high RH conditions, LWC accounts for a certain proportion of particles (Jia and Xu, 2018). To obtain the time evolution of SOA concentrations, the LWC has to be subtracted during the whole photooxidation period. Since LWC was only measured at the end of the reaction, the volume growth factor (VGF) was used to estimate the contribution of LWC in particles, which was defined as the ratio of the humid particle volume to the dry particle volume (Engelhart et al., 2011). It was assumed that the VGF did not change during the whole photooxidation period. Thus, the LWC can be obtained by VGF. As shown in Fig. 1, the wall-loss-corrected SOA mass concentrations are plotted as a function of photooxidation reaction time for *m*-xylene-OH systems at different RHs. The removal of aerosol water during the LWC measurement may cause the dissolved species that are probably volatile/ semi-volatile compounds to evaporate back into the gas phase. Glyoxal is a typical semi-volatile compound with high Henry's law constant, which is involved in SOA formation in *m*-xylene-OH system of our study. The Henry's law constant of glyoxal in pure water is as high as $4.19 \times 10^5 \text{ M atm}^{-1}$ at 298 K (Ip et al., 2009). Only one in ten thousand of glyoxal can dissolve in the LWC whose

concentration was obtained in our study. Thus, SOA concentrations for intermediate and high RH conditions were slightly underestimated, but the underestimation is extremely low and can be negligible.

It can be clearly observed that there is a large difference in the maximum mass concentration between low and high RHs. The maximum mass concentrations fitted are 150.3 and 95.5 $\mu\text{g m}^{-3}$ at low RHs, whereas they are 21.0 and 7.5 $\mu\text{g m}^{-3}$ at high RHs, with the largest difference being over ten times. The RH effect was reproducible when the initial *m*-xylene concentration was changed under similar conditions. To obtain the particle mass concentrations and SOA yield, an SOA density of 1.4 g cm^{-3} was used (Song et al., 2007). The fairly large scatter in the mass concentrations of SOA in Fig. 1 was observed, which mainly results from the uncertainty of SOA measurement by SMPS instrument. The interval of SOA data sampled by SMPS was 5 minutes, for which the sampling frequency was relatively low. Technically, according to the instruction manual of the CPC (Model 3776), the particle concentration accuracy is $\pm 10\%$ at $< 3 \times 10^5$ particles cm^{-3} . The number concentrations at the end of each experiment in this study were below 5×10^3 particles cm^{-3} , so in this study the particle concentration error caused by CPC alone was $\pm 10\%$. In addition, size-dependent aerosol charging efficiency uncertainties and CPC sampling flow rate variability also dominate the SMPS measurement uncertainty. The combination of various uncertainties, including SMPS measurement, sampling and even conversion of mass concentration from number concentration leads to the fairly large scatter in Fig. 1.

We used the definition of the ratio of the SOA mass to the consumed *m*-xylene mass to calculate the SOA yield at the end of each experiment. As summarized in Table 1, the SOA yields at low RH are 14.0-14.6%, while those at high RH are only around 0.8-2.5%. Both mass concentrations and SOA yields at low RH are an order of magnitude larger than those at high RH. Though temperatures at high RH are slightly higher than those at low RH as shown in Table 1, which can lead to a higher SOA yield, the difference of temperatures between low and high RH conditions is lower than two degree, which cannot lead to a significantly different SOA yield to affect the result (Qi et al., 2010).

Seed aerosols were not artificially introduced throughout all the experiments, which could lead to the underestimation of SOA, as SOA-forming vapors partly condense to the reactor walls instead of particles (Matsunaga and Ziemann, 2010; Zhang et al., 2014). The extent to which vapor wall deposition affects SOA mass yields depends on the specific parent hydrocarbon system (Zhang et al., 2014; Zhang et al., 2015; Nah et al., 2016; Nah et al., 2017). Zhang et al (2014) have estimated two *m*-xylene systems under low NO_x conditions and concluded that SOA mass yields were underestimated by factors of 1.8 (Ng et al., 2007) and 1.6 (Loza et al., 2012) under low RH conditions. In addition, the excess use of H_2O_2 can lead to an excess OH radicals, leading to a less underestimation of SOA formation as the losses of SOA-forming vapors can be mitigated via the use of excess oxidant concentrations (Nah et al., 2016). Thus, the underestimation of SOA formation can be limited. In fact, the wall loss of *m*-xylene was not taken into consideration of calculation of mass yields, which generally overestimates the mass yields.

The wall loss of chemical species that is sensitive to humidity may affect the RH effect on SOA yields, as the reduction of SOA yields at the high humidity may be due to the chemical loss to the wet reactor wall. To estimate the extent of how much the wall loss of chemical species affects the SOA formation at different RHs, we take glyoxal and acetone as reference

compounds. Glyoxal, a typical compound that can form SOA, can easily dissolve in the aqueous phase due to the large Henry's law constant of $4.19 \times 10^5 \text{ M atm}^{-1}$ at 298 K (Ip et al., 2009), very sensitive to humidity. Loza et al. (2010) found that the wall loss of glyoxal was minimal at 5% RH, with $k_w = 9.6 \times 10^{-7} \text{ s}^{-1}$, whereas k_w was $4.7 \times 10^{-5} \text{ s}^{-1}$ at 61% RH. We assume that k_w linearly increases with RH, and the k_w value is estimated to be $6.1 \times 10^{-5} \text{ s}^{-1}$ at 80% and 7.4×10^{-6} at 13%
5 RH, with the difference being 8.2 times. According to the wall loss of glyoxal, glyoxal only decreased by 10% at the end of our experiment at low RH, while glyoxal decreased by 59% at high RH. Acetone can hardly dissolve in the aqueous phase due to the small Henry's law constant of 29 M atm^{-1} (Poulain et al., 2010), which is 4 orders of magnitude less than that of glyoxal. Ge et al. (2017) obtained that the wall loss of acetone was $5.0 \times 10^{-6} \text{ s}^{-1}$ at 87% RH and $3.3 \times 10^{-6} \text{ s}^{-1}$ at 5% RH, with a factor of 1.5. The difference of wall loss between glyoxal and acetone at low RH is about 2 times, while it becomes about
10 12 times at high RH. Thus, it can be considered that the wall loss among different species at low RH is less affected by the Henry's law constant, but it is greatly affected at high RH. In our study glycolaldehyde (See the Sec. 3.4) is proposed to be an important SOA precursor that can form a large fraction of oligomers in our experiments, but the wall loss of glycolaldehyde is not available. The Henry's law constant of glycolaldehyde was obtained to be $4.14 \times 10^4 \text{ M atm}^{-1}$ (Berterton and Hoffmann, 1988), an order of magnitude lower than glyoxal, indicating that glycolaldehyde is less sensitive to
15 humidity than glyoxal but much more sensitive to humidity than acetone. Based on the data of these two reference species, the wall loss of glycolaldehyde at low RH is taken to be $5 \times 10^{-6} \text{ s}^{-1}$, and the difference in wall loss between high and low RHs is about 6 times. Then, the wall loss of glycolaldehyde at high RH can be $3 \times 10^{-5} \text{ s}^{-1}$. Then, it is estimated that glycolaldehyde would decrease by 7% at low RH and by 35% at high RH at the end of our experiment, respectively. This means that SOA yield would be underestimated by 35% at high RH and by 7% at low RH if glycolaldehyde lost to the wall
20 was completely transformed to SOA. If this wall effect of SOA precursors was taken into consideration, the SOA yields at high (Exp. 6) and low (Exp. 2) RHs would be 3.4% and 15.1%, respectively. Alternatively, the SOA yield at high RH was underestimated to be 42% relative to that at low RH. Even the sensitivity of the wall loss to RH was taken to be 8 times, the SOA yield at high RH would be underestimated to be 62% compared to that at low RH. In fact, there were many different SOA precursors from the *m*-xylene oxidation system that probably have much smaller Henry's law constant relative to that
25 of glycolaldehyde. Thus, it is concluded that the RH effect on SOA formation from *m*-xylene photooxidation by H_2O_2 is negative.

For comparison and discussion of the results of SOA formation with other previous studies, Fig. 2 was plotted to show the SOA yields as a function of RH for the different aromatic (toluene and *m*-xylene) oxidation under low NO_x conditions with the photolysis of H_2O_2 as the OH source. In Fig. 2, the hollow circles represent that no seed particles were introduced and the circles with a cross represent that seed particles were introduced, and the size of markers indicates the magnitude of amount
30 of reacted VOC. In the most recent study on toluene SOA formation conducted without seed particles (Hinks et al., 2018), the SOA yield at low NO_x level was 15% under dry conditions (< 2% RH) and 1.9% under humid conditions (89% RH), with the ratio of two yields between dry and humid conditions being over 7.5. The toluene SOA produced under high RH conditions were significantly suppressed, in which the tendency of RH effects on SOA yield was very similar with our study,

though the difference of SOA yield in the range of low and high RH conditions in Hinks et al (2018) was slightly smaller than that in this study. The small difference of RH effects between Hinks et al. and our study is likely associated with the difference in experimental conditions, including RHs, initial and reacted VOCs and H₂O₂ concentrations, in addition to different species. This comparison demonstrates that different species of toluene and *m*-xylene of aromatics pose very similar RH effects under low-NO_x conditions. Hinks et al. attributed the suppression of SOA yields by elevated RH to the lower level of oligomers generated by condensation reactions and the reduced mass loading at high RH. In a study on an SOA model for toluene oxidation, the negative RH effect on SOA formation was also found in the presence of seed particles (Cao and Jang, 2010). In their study, the SOA yield at low NO_x level was 28-30% under low RH conditions (17-18% RH) and 20-25% under moderate RH conditions (48% RH) (Cao and Jang, 2010), but they did not focus on the RH effect to give an explanation. Furthermore, their RH only changed from 17% to 48%, the reacted parent VOC was smaller and the seed particles were present, so the RH effect on SOA yields was not as significant as those in Hinks et al and our study. Ng et al. have investigated the yields of SOA formed from *m*-xylene-OH system at low RH (4-6%) under low NO_x conditions (Ng et al., 2007). They obtained that the SOA yields were in the range of 35.2-40.4% in the presence of seed particles. The SOA yields were larger than those of our study, as they conducted the experiments under different irradiation time and with inorganic seed particles. These seed particles can provide not only surface for chemical reactions, but also acidic and aqueous environments that can promote the SOA formation (Jang et al., 2002; Liu et al., 2018; Faust et al., 2017). The reacted concentration of parent VOC was close between Cao and Jang and Ng et al. though the species were different. The results from these two studies can be considered together, since their experiments all had seed particles. As shown in Fig. 2, the obviously negative RH effect on SOA yields can be found. In addition to these three previous studies shown in Fig. 2, a study on chemical oxidative potential of SOA (Tuet et al., 2017) found that the concentration of SOA from *m*-xylene irradiation at low NO_x level under dry condition was much larger than that under humid condition (89.3 μg m⁻³ at < 5% RH and 13.9 μg m⁻³ at 45% RH), but they did not calculate the *m*-xylene SOA yields or give an explanation for the RH effect.

4. Page 5, line 20. Why did the authors stop the experiments after 4h, while the SOA mass was still increasing? Usually, SOA yields are calculated when the oxidation of the precursor is over. Was H₂O₂ still present in the chamber?

As the referee pointed out, the SOA mass was still increasing after 4 h. The experiment for 4-6 h is a ubiquitous reaction time used in many previous studies. The SOA yield indeed generally increases with time. H₂O₂ was still present in the chamber after 4 h. If the relationship between the yield and time is extrapolated to 6 h, the yield will be increased by 45% relative to that at 4 h (Exp. 1), which can be compared with many previous studies (Cao and Jang, 2010; Hinks et al., 2018). Most importantly, as the purpose of our study is to investigate the RH effect on SOA formation, the reaction time of 4 h is sufficient to compare the SOA formation and to sample for SOA component analysis. Furthermore, a relatively short reaction time can minimize the wall loss of oxidized species and limit the further SOA mass uncertainty.

Cao, G., and Jang, M.: An SOA model for toluene oxidation in the presence of inorganic aerosols, *Environ. Sci. Technol.*, 44, 727-733, 10.1021/es901682r, 2010.

Hinks, M. L., Montoya-Aguilera, J., Ellison, L., Lin, P., Laskin, A., Laskin, J., Shiraiwa, M., Dabdub, D., and Nizkorodov, S. A.: Effect of relative humidity on the composition of secondary organic aerosol from the oxidation of toluene, *Atmos. Chem. Phys.*, 18, 1643-1652, 10.5194/acp-18-1643-2018, 2018.

5 Page 5, lines 25-27; 30-32. I do not think it is a correct explanation. Indeed, as reported in many laboratory studies, SMPS measurements are reliable and do not exhibit such a large variability (15-20%). The authors should better constrain the evaluation of the uncertainties and provide references supporting their hypothesis.

10

We agree with the referee that in many studies SMPS measurements do not exhibit the variability as large as in our study. However, there are also some studies with such a large variability of SMPS measurement. For example, Sakamoto et al. (2013) found a large uncertainty (~20% or even more, the ratio of standard deviation to mean value) within 2.5 min when measuring particulate volume concentration. Technically, according to the instruction manual of the ultrafine condensation particle counter (Model 3776), the particle concentration accuracy is $\pm 10\%$ at $< 3 \times 10^5$ particles cm^{-3} . The number concentrations at the end of each experiment in this study were below 5×10^3 particles cm^{-3} , so in this study the particle concentration error caused by CPC alone was $\pm 10\%$. As can be seen in Fig. S2, the particle distribution falls into two particle diameter ranges. Here take Exp.1 as an example to explain, 130.0-371.8 nm and 461.4-661.2 nm. For evaluation of the uncertainty of the mass concentration, we assume that if the 10% uncertainty of number concentration exists in the particle diameter range of 461.4-661.2 nm (Exp. 1), the uncertainty of mass concentration would be 17%. This is more likely to happen in this study as the number concentration is extremely lower than that in many other studies (10^4 - 10^5 particles cm^{-3} order of magnitudes), in which the seed particle was used or the background air was not clean enough with the presence of SO_2 . In addition, size-dependent aerosol charging efficiency uncertainties and CPC sampling flow rate variability also dominate the SMPS measurement uncertainty. The combination of various uncertainties, including SMPS measurement, sampling and even conversion of mass concentration from number concentration leads to the fairly large scatter in Fig. 1. Based on the reply above, we have rewritten the explanation in the revised manuscript.

15

20

25

Sakamoto, Y., Inomata, S., and Hirokawa, J.: Oligomerization reaction of the Criegee intermediate leads to secondary organic aerosol formation in ethylene ozonolysis, *J. Phys. Chem. A*, 117, 12912-12921, 10.1021/jp408672m, 2013.

30

The interval of SOA data sampled by SMPS was 5 minutes, for which the sampling frequency was relatively low. Technically, according to the instruction manual of the CPC (Model 3776), the particle concentration accuracy is $\pm 10\%$ at $< 3 \times 10^5$ particles cm^{-3} . The number concentrations at the end of each experiment in this study were below 5×10^3 particles cm^{-3} , so in this study the particle concentration error caused by CPC alone was $\pm 10\%$. In addition, size-dependent aerosol

charging efficiency uncertainties and CPC sampling flow rate variability also dominate the SMPS measurement uncertainty. The combination of various uncertainties, including SMPS measurement, sampling and even conversion of mass concentration from number concentration leads to the fairly large scatter in Fig. 1.

- 5 6. Page 6, line 5. How did the authors conclude that the underestimation was negligible? Please provide a clear explanation.

The underestimation comes from the dissolved species that are probably volatile/semi-volatile compounds to evaporate back into the gas phase when aerosol water is removed. Glyoxal is a typical semi-volatile compound that is involved in SOA formation in *m*-xylene-OH system of our study. We will take glyoxal as the example to interpret why the underestimation was negligible. The LWC after 4 h from the start of reaction in Exp. 7 which was under the highest RH condition was $4.4 \mu\text{g m}^{-3}$ as shown in Table 1. According to the MCM prediction, the final concentration of glyoxal during the 4 h of experiment time is 17 ppb. The Henry's law constant of glyoxal in pure water is $4.19 \times 10^5 \text{ M atm}^{-1}$ at 298 K (Ip et al., 2009). The glyoxal dissolved in the LWC can be calculated to be less than 1 ppt. Thus, the evaporation of the volatile/semi-volatile compounds back to the gas phase can be negligible. In addition, growth factor (GF) was determined to be 1.2 in Exp. 7 of our study. Aklilu and Mozurkewich (2004) gave a GF range of 1.05–1.12 for atmospheric organic particles (79% RH). Cocker et al (2001) reported the GF of 1.14 at 85% RH for SOA formed from *m*-xylene. In general, our results of GF are in good agreement with previous studies, indicating that the LWC measured by our modified SMPS is reliable. Though the removal of aerosol water may cause the dissolved species that are probably volatile/semi-volatile compounds to evaporate back into the gas phase, which may lead to the underestimation of SOA, it can be negligible. Thus, we have added some sentences in the first paragraph in the Sec. 3.1 in the revised manuscript.

- Aklilu, Y. A. and Mozurkewich, M.: Determination of external and internal mixing of organic and inorganic aerosol components from hygroscopic properties of submicrometer particles during a field study in the lower fraser valley, *Aerosol Sci. Tech.*, 38, 140-154, 10.1080/02786820490251367, 2004.
- 25 Cocker, D. R., Mader, B. T., Kalberer, M., Flagan, R. C., and Seinfeld, J. H.: The effect of water on gas-particle partitioning of secondary organic aerosol: II. *m*-xylene and 1,3,5-trimethylbenzene photooxidation systems, *Atmos. Environ.*, 35, 6073-6085, 10.1016/s1352-2310(01)00405-8, 2001.
- Engelhart, G. J., Hildebrandt, L., Kostenidou, E., Mihalopoulos, N., Donahue, N. M., and Pandis, S. N.: Water content of aged aerosol, *Atmos. Chem. Phys.*, 11, 911-920, 10.5194/acp-11-911-2011, 2011.
- 30 Ip, H. S. S., Huang, X. H. H., and Yu, J. Z.: Effective Henry's law constants of glyoxal, glyoxylic acid, and glycolic acid, *Geophys. Res. Lett.*, 36, L01802, 10.1029/2008gl036212, 2009.

Glyoxal is a typical semi-volatile compound with high Henry's law constant, which is involved in SOA formation in *m*-xylene-OH system of our study. The Henry's law constant of glyoxal in pure water is as high as $4.19 \times 10^5 \text{ M atm}^{-1}$ at 298 K

(Ip et al., 2009). Only one in ten thousand of glyoxal can dissolve in the LWC whose concentration was obtained in our study.

5 Ip, H. S. S., Huang, X. H. H., and Yu, J. Z.: Effective Henry's law constants of glyoxal, glyoxylic acid, and glycolic acid, *Geophys. Res. Lett.*, 36, L01802, 10.1029/2008gl036212, 2009.

7. Page 6, lines 20-28. To help the reader and underline the differences, the authors should make a figure presenting the SOA yields as a function of RH for the different aromatic systems (toluene, xylene,...). It would help picturing the effect of RH. In addition, they can use the size of the markers as the function of reacted VOC as the concentration of reacted VOC has a great
10 impact on SOA yields.

Taking the referee's suggestion, we have made the figure and added it to the revised manuscript as Figure 2. Also, we have added some sentences about this figure in the last paragraph of the Sec. 3.1 in the revised manuscript which can be seen in the reply of comment 3.

15

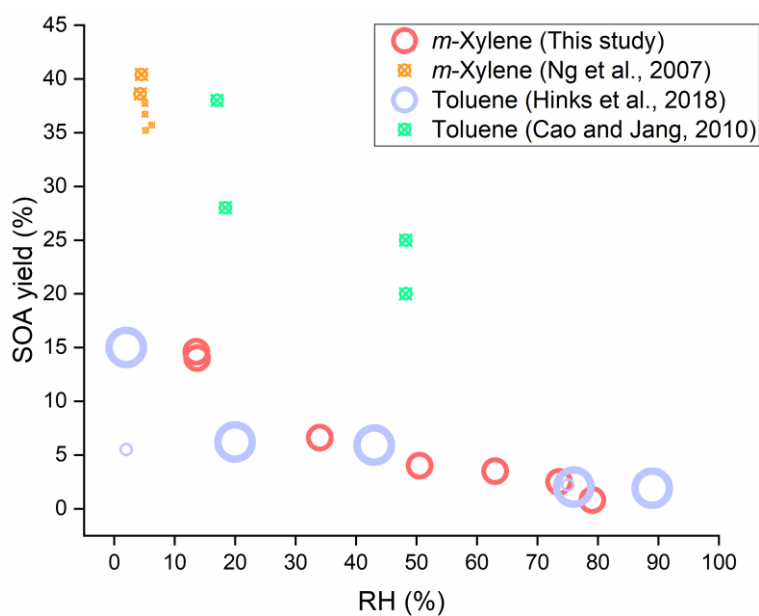


Figure 2. SOA yields as a function of RH for the different aromatic (toluene and *m*-xylene) oxidation under low NO_x conditions with the photolysis of H₂O₂ as the OH source. The hollow circles represent that no seed particles were introduced and the circles with a cross represent that seed particles were introduced. The size of markers indicates the magnitude of
20 amount of reacted VOC.

8. Page 8, lines 23-25. Please provide references to support the assignments. if the band at 1605 cm⁻¹ corresponds to liquid water, why is the absorption lower in humid conditions when the LWC is expected to be larger?

5 Taking the referee's suggestion, we have added references to support the assignments in the second paragraph of Sec. 3.2 in the revised manuscript. In addition, we corrected the mistake about the assignment of the band at 1605 cm⁻¹ in the revised manuscript. In fact, the sample compartment of the FTIR spectrometer was purged by dry air desiccated from FTIR purge gas generator (Model 75-45-12VDC, Balston, Parker) ahead of the FTIR measurement. The dew point temperature of the dry gas from this generator is as low as -65 °C, so the RH of the environment inside the FTIR spectrometer was extremely low, close to zero when FTIR spectra were obtained. The band at 1605 cm⁻¹ should be C-C stretching of aromatic rings and the
10 C=O stretching of conjugated carbonyl groups.

The broad absorption at 3600-2400 cm⁻¹ is O-H stretching vibration in phenol, hydroxyl and carboxyl groups (Stevenson and Goh, 1971; Santos and Duarte, 1998; Duarte et al., 2005). The band at 3000 cm⁻¹ is C-H stretching vibration (Stevenson and Goh, 1971; Santos and Duarte, 1998; Duarte et al., 2005). The sharp absorption at 1720 cm⁻¹ is the C=O stretching vibration
15 in carboxylic acids, formate esters, aldehydes and ketones (Stevenson and Goh, 1971; Santos and Duarte, 1998; Duarte et al., 2005). The absorptions at 1605 cm⁻¹ match C-C stretching of aromatic rings and the C=O stretching of conjugated carbonyl groups. The absorptions at 1415 cm⁻¹ match the deformation of CO-H, phenolic O-H and C-O (Coury and Dillner, 2008; Ofner et al., 2011). The absorptions at 1180 cm⁻¹ match the C-O-C stretching of polymers, C-O and OH of COOH groups (Jang and Kamens, 2001; Jang et al., 2002; Duarte et al., 2005). The absorptions at 1080 cm⁻¹ match the C-C-OH stretching
20 of alcohols (Jang and Kamens, 2001; Jang et al., 2002).

Coury, C., and Dillner, A. M.: A method to quantify organic functional groups and inorganic compounds in ambient aerosols using attenuated total reflectance FTIR spectroscopy and multivariate chemometric techniques, *Atmos. Environ.*, 42, 5923-5932, 10.1016/j.atmosenv.2008.03.026, 2008.

25 Duarte, R. M. B. O., Pio, C. A., and Duarte, A. C.: Spectroscopic study of the water-soluble organic matter isolated from atmospheric aerosols collected under different atmospheric conditions, *Analytica Chimica Acta*, 530, 7-14, 10.1016/j.aca.2004.08.049, 2005.

Jang, M., Czoschke, N. M., Lee, S., and Kamens, R. M.: Heterogeneous atmospheric aerosol production by acid-catalyzed particle-phase reactions, *Science*, 298, 814-817, 10.1126/science.1075798, 2002.

30 Jang, M. S., and Kamens, R. M.: Characterization of secondary aerosol from the photooxidation of toluene in the presence of NO_x and 1-propene, *Environ. Sci. Technol.*, 35, 3626-3639, 10.1021/es010676+, 2001.

Ofner, J., Kruger, H.-U., H., G., Schmitt-Kopplin, P., Whitmore, K., and Zetzsch, C.: Physico-chemical characterization of SOA derived from catechol and guaiacol-a model substance for the aromatic fraction of atmospheric HULIS, *Atmos. Chem. Phys.*, 11, 1-15, 10.5194/acp-11-1-2011, 2011.

Santos, E. B. H., and Duarte, A. C.: The influence of pulp and paper mill effluents on the composition of the humic fraction of aquatic organic matter, *Wat. Res.*, 32, 597-608, 10.1016/S0043-1354(97)00301-1, 1998.

Stevenson, F. J., and Goh, K. M.: Infrared spectra of humic acids and related substances, *Geochim. Cosmochim. Acta*, 35, 471-483, 10.1016/0016-7037(71)90044-5, 1971.

5

9. Page 8, lines 29-30. Are the ratio calculated for 1 experiment or for all the experiments?

The ratio was not calculated for all experiments but using the results from Exps. 2 and 6. According to the comment 1 of referee 4, we have added three experiments and we renew the serial number of each experiment as shown in Table 1. For clear statement of how we calculated the ratio, we have added the serial numbers of low and high experiments to the first sentence in paragraph 2 and the second sentence in paragraph 3 of Sec. 3.2, as well as the title of Table 2.

10

The assignment and the intensity of the FTIR absorption frequencies at low (Exp. 2) and high (Exp. 6) RHs is summarized in Table 2.

15

As well, Table 2 gives the ratio of intensities at high RH (Exp. 6) to those at low RH (Exp. 2) to compare the difference of relative intensities of functional groups.

Table 2. Absorbance positions of functional groups and the intensities at low (Exp. 2) and high (Exp. 6) RHs.

20

10. Page 9, lines 15-16. Please provide the MS² spectra in the SI to support the discussion and the structure assignments.

Taking the referee's suggestion, we have added the MS² spectra in Figure S3 and the breakage mechanism in Fig. S4 of the Supporting Information.

25

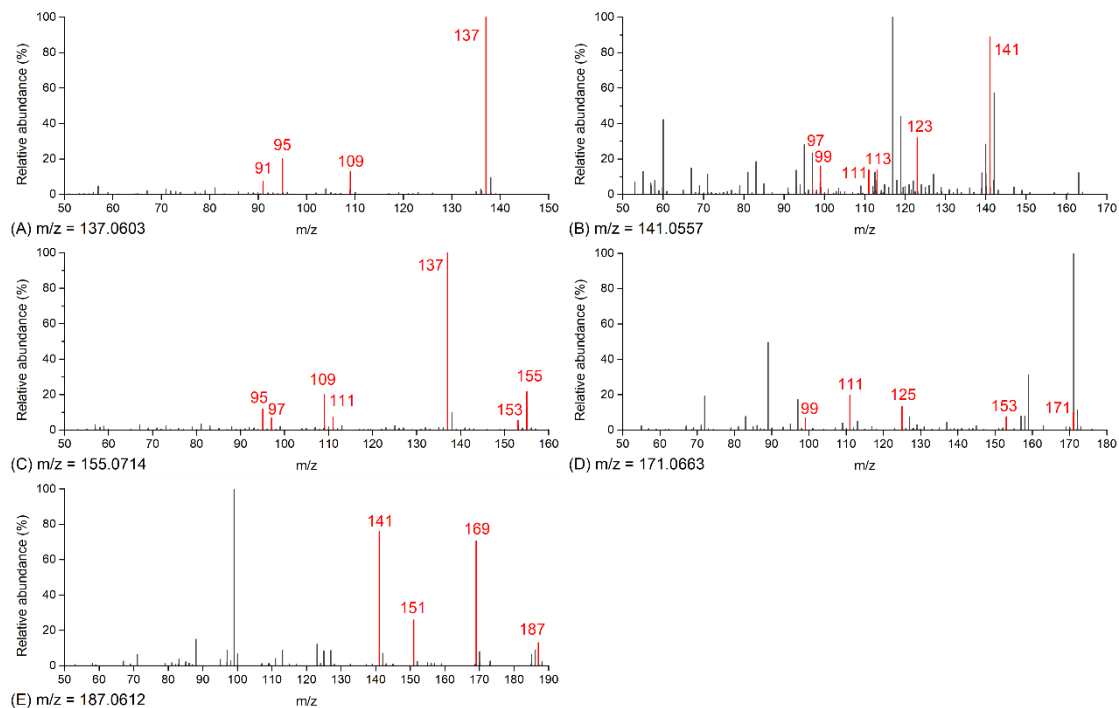
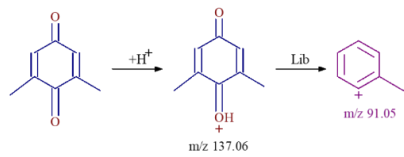
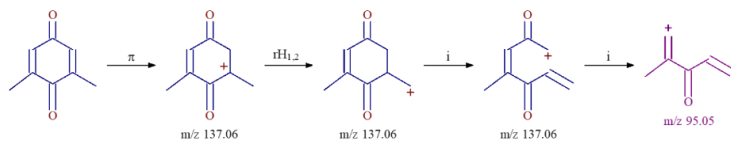
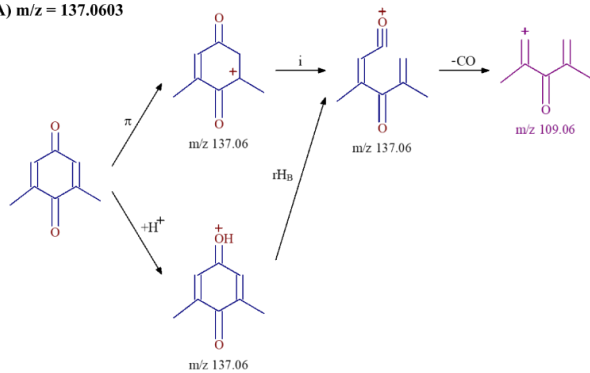


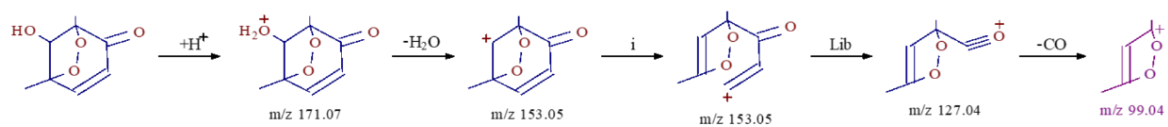
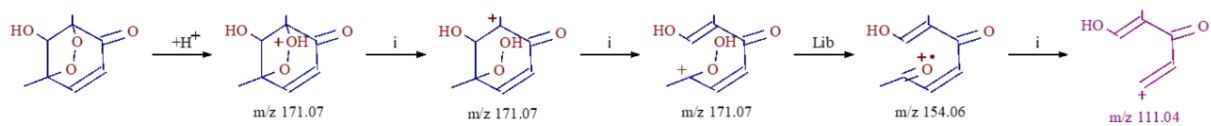
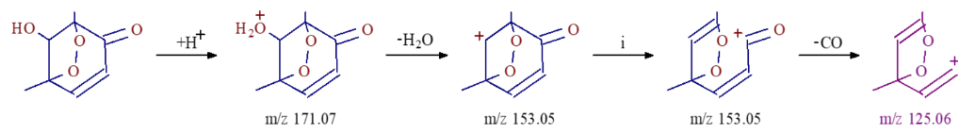
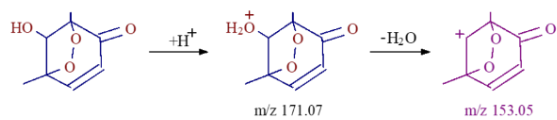
Figure S3. MS² spectrum of the parent ion at m/z = 137 (A), m/z = 141 (B), m/z = 155 (C), m/z = 171 (D) and m/z = 187 (E) in Table 3. The red columns are the main fragments those are matched with the fragments proposed by the Mass Frontier program.

5

(A) $m/z = 137.0603$



(D) $m/z = 171.0663$



(E) $m/z = 187.0612$

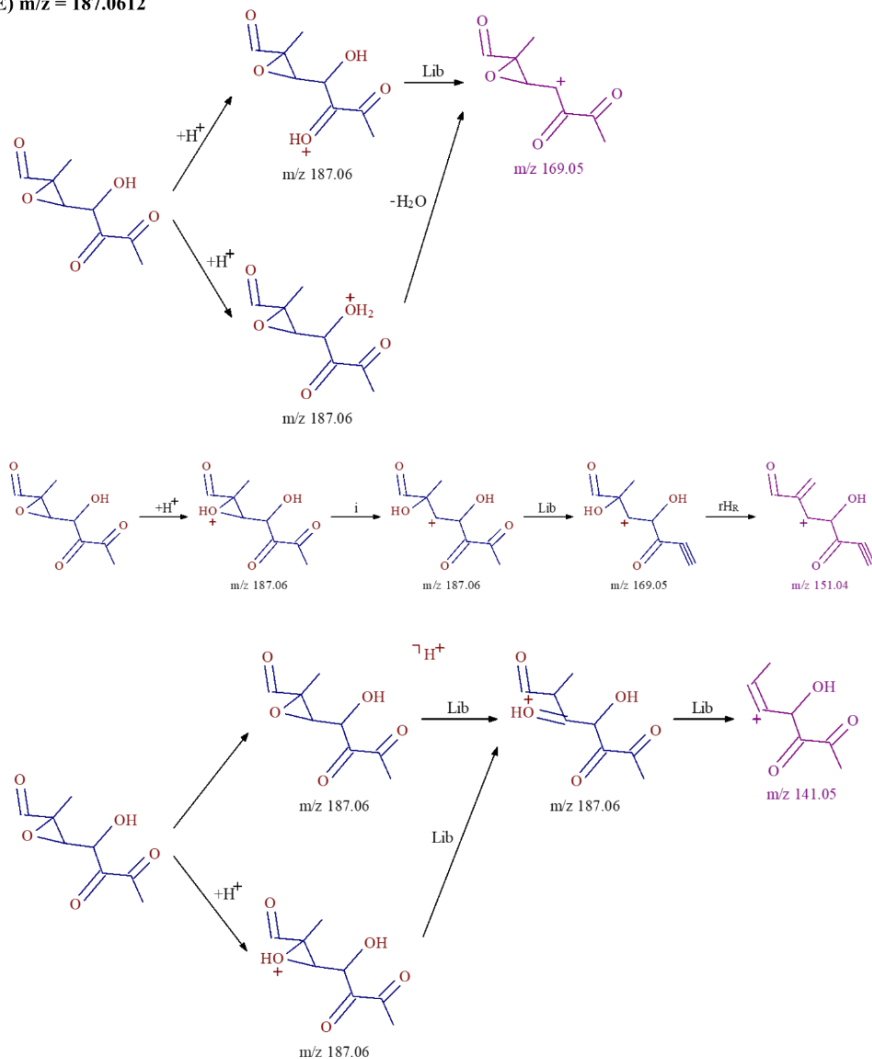


Figure S4. Breakage mechanisms of the parent ion at $m/z = 137$ (A), $m/z = 141$ (B), $m/z = 155$ (C), $m/z = 171$ (D) and $m/z = 187$ (E) in HRMS, proposed in the Mass Frontier program. The process symbols of Lib, i and rH represent the pathway from the HighChem Fragmentation Library, the pathway of inductive cleavage, and the charge site rearrangement.

5

11. Page 9, line 24. It would be very surprising to have such reactive species (e.g., 155, 187) within the particle phase. Please provide much deeper MS2 analyses to further confirm the presence of such species and add references.

MS² spectra of $m/z=155$ and 187 have been added in Fig. S3 in the Supporting Information. The formula of $m/z = 155$ and 187 in positive ion mode are identified to be $C_8H_{10}O_3$ and $C_8H_{10}O_5$, respectively. The rate constants of reaction of $C_8H_{10}O_3$

10

and $C_8H_{10}O_5$ with OH are 8×10^{-11} and $4 \times 10^{-11} \text{ cm}^3 \text{ molecule}^{-1} \text{ s}^{-1}$ in the MCM, with a factor of 4 and 2 compared with that of *m*-xylene with OH, respectively. According to the MCM prediction, the concentration of these two compounds in the gas phase can reach 20 and 8 ppb respectively during the reaction process. In other words, though these two compounds are relatively reactive, they can still partition in the particle phase. In addition, the formation pathways of the MS^2 fragment of $m/z=155$ and 187 proposed by the Mass Frontier program are shown in the Fig. S4 in the supporting information, as can be seen in the reply of comment 10.

12. Page 10, lines 1-5. The most intense peak corresponds to C10 compounds, so according to the author's definition, those compounds are oligomers. It is surprising that oligomers (dry conditions, no seed) contribute to a large fraction of SOA mass. Indeed, larger SOA mass would result in a larger aerosol surface area and lead to a greater condensation sink for SVOC and LVOC. In other words, it can be expected that larger SOA formation leads to a greater concentration of SVOC (i.e., monomer) within the particle phase. Please provide a deeper analysis of gas-particle partitioning in your experiments: what's the surface area of the aerosols under dry vs wet conditions and compare it with the surface area of the wall. Under dry conditions the aerosol would act as a main sink, while under wet conditions the chamber walls would be the main sink.

Indeed, as can be seen in Fig. 5, the compounds with lower nC ($nC=4-7$) in the particle phase were observed at low RH but not at high RH. In other words, more compounds with high volatility are condensed in the particle phase at low RH. The surface area of the reactor wall was 6.6 m^2 . At 4 h of Exps. 1 and 7, the surface concentrations of the aerosols were 1.01×10^9 and $1.25 \times 10^8 \text{ nm}^2 \text{ cm}^{-3}$ at low and high RHs, respectively. The ratio of the aerosol surface area to the surface area of the wall was 1.5×10^{-4} and 1.9×10^{-5} at low and high RHs, respectively. If the chamber wall were the main sink at high RH, particles at low RH could be also lost on the chamber wall. Thus, some chemical processes must dominate the negative RH effect on SOA formation other than gas to particle partitioning. In addition, the comment about the C10 compounds is closely related to the next comment, so please see the reply of the next comment.

13. Page 10, line 15. What should be the production of glycolaldehyde to explain the formation/concentration of such high molecular weight compounds? It is confusing to not see any dimers and/or lower oligomers ($nC = 3,4,5,\dots$ monomers). In other words, the authors are suggesting that from gaseous glycolaldehyde, such aldol condensation reaction will form only/mainly oligomers with 8 monomers. If such a process takes place the authors should be able to find the distribution of the different oligomers. Is it the case? The authors should look at the MS/MS spectra of the compounds from C4 to C10 to look for the presence of oligomers ($nC = 3,4,5,\dots$). The MS/MS spectra should be provided. Is there any evidence of oligomerization between a xylene-monomer and a carbonyl (e.g., glycolaldehyde)? Finally, such aldol processes are generally considered to be too slow to be observed, especially without the presence of an acidic solution (Herrmann et al., 2015).

We went through the MS² spectra of C4-C9 compounds and did not find any C₂H₅O₂ fragment that is generally identified as glycolaldehyde. We agree with the referee that the formation of oligomers with glycolaldehyde part would not only be in C10 compounds. The C10 compounds may not be from the oligomerization of glycolaldehyde and monomers. So we have deleted the explanation of C10 compounds in the revised manuscript.

5

14. Have the authors considered the reaction of glycolaldehyde with C7-C8 monomers?

We considered the reaction of glycolaldehyde with C8 monomers as the Comment 13 mentioned, but we did not consider the reaction of glycolaldehyde with C7 monomers, since we did not find any C₂H₅O₂ fragment in C9 compounds in MS² spectra, as we replied the Comment 13. Thus, the C₂H₅O₂ fragment in C10 compounds cannot be considered as glycolaldehyde.

10

15. Paragraph 3.4. This section is incorrect and should be revised according to the existing literature on HOM. The authors characterized the distribution of oxygenated species in particle phase as a function of RH. According to Bianchi et al., 2019, HOM refer to gas-phase highly oxygenated molecules formed from autoxidation. So it is speculative to claim that RH impacts HOM formation as the authors did not measure such species. In addition, it is contradicting a recent study proposed by Li et al. 2019 (doi.org/10.5194/acp-19-1555-2019) showing that RH does not impact the formation of HOM. It is possible that HOM undergo further particle-phase reactions as it has been suggested in a few studies (i.e., Bianchi et al., 2019).

15

Taking the referee's advice, we have modified Sec. 3.4 in the revised manuscript.

20

The large difference of SOA yields and composition between low and high RHs is proposed that water is directly involved in the chemical mechanism and further affects the SOA growth. In the particle-phase accretion equilibrium reactions, where water is involved as a by-product, the elevated RH alters the equilibrium of reaction by moving toward reducing the fraction of oligomers with low volatility and increasing the fraction of monomers (Nguyen et al., 2011; Hinks et al., 2018). In this study and the previous study on toluene SOA formation, C₂H₂O was one of the most frequent mass difference at low and high RHs, but the peak intensities of its related compounds were much lower under elevated RH conditions (Hinks et al., 2018). C₂H₂O was proposed to be from the oligomerization reaction of glycolaldehyde (C₂H₄O₂), which can react with carbonyl compounds by aldol condensation reactions with water as the by-product. This chemistry may dominantly affect the negative RH effect on the whole process of SOA formation.

25

Moreover, there may exist other processes that enlarge the difference of SOA formation under various RH conditions. Before we discuss the possible processes, the reaction pathway between *m*-xylene and OH radicals need to go through first. Reactions between *m*-xylene (C₈H₁₀) and OH radicals have two pathways, the H-abstraction from the methyl group and OH-addition to the aromatic ring, which generates products such as methylbenzaldehyde (C₈H₈O) and methylbenzyl alcohol (C₈H₁₀O), as shown in Scheme 1. OH-addition is the dominant pathway, as the branching ratio of H-abstraction only

30

accounts for 4% based on MCM. OH-addition to the aromatic ring is followed by O₂-adduct and isomerization to form a carbon-centered radical, which can form a dimethylphenol (C₈H₁₀O) or is adducted by an O₂ molecule forming a bicyclic peroxy radical (BPR, C₈H₁₁O₅) (Calvert et al., 2002; Birdsall et al., 2010; Wu et al., 2014). The BPR reacts with other RO₂ radicals or HO₂ forming the bicyclic oxy radical (C₈H₁₁O₄). This RO radical can get further reaction and finally form
5 carbonylic products, such as (methyl) glyoxal and other SOA precursors (Jenkin et al., 2003; Hallquist et al., 2009; Carlton et al., 2010; Carter and Heo, 2013), or react with HO₂ radicals forming bicyclic hydroxyhydroperoxides (ROOH, C₈H₁₂O₅), or react with other RO₂ radicals forming ROH (C₈H₁₂O₄) and R-HO (C₈H₁₀O₄). The self- and cross-reactions of RO₂ radicals also form ROOR (C₁₆H₂₂O₁₀) or ROOR' that is the accretion products (Berndt et al., 2018; Molteni et al., 2018). The further O₂-adduct of BPR can form a highly-oxygenated RO₂ radicals and further get reacted and finally form highly oxygenated
10 organic molecules (HOMs) (Types 1 and 2 in Scheme 1) (Wang et al., 2017; Crouse et al., 2013; Ehn et al., 2014; Jokinen et al., 2015; Berndt et al., 2016). Dimethylphenol (C₈H₁₀O) as well as other products from termination reaction with benzene ring or double bond can react with OH radicals and get further reacted to form HOMs as well.

Most of HOMs can fall into extremely low or low volatility organic compounds ((E)LVOC) and a small number of HOMs are semi-volatility organic compounds (SVOC) (Bianchi et al., 2019). ELVOCs can condense onto particles but SVOCs
15 exist in significant fractions in both the condensed and gas phases at equilibrium. As SMPS measured, at the end of the experiment the number concentrations (not corrected) of Exp. 1 (low RH) and Exp. 7 (high RH) were 1.9×10^3 and 5.8×10^2 particles cm⁻³, with a factor of 3; while the mass concentrations (not corrected) of Exp. 1 (low RH) and Exp. 7 (high RH) were 116.9 and 8.7 μg m⁻³, with a factor of 13. This indicates that the size of particles at low RH are higher than that at high RH. The O:C ratios in positive and negative ion modes under low and high RH conditions were roughly calculated using the
20 carbon and oxygen atom numbers multiplied by the relative intensities obtained by HRMS. The O:C ratio in the positive ion mode was close to each other, 0.56 and 0.58 at low and high RHs, respectively; while the O:C ratio in the negative ion mode was differential, 0.66 and 0.77 at low and high RHs, respectively. Based on the gas to particle partitioning rule, the more volatile compounds in the gas phase can condense to the particles with larger size (Li et al., 2018). It can be deduced that the particles with larger size at the reduced RH result in more SVOC in the gas phase to condense, leading to the difference of
25 SOA mass at various RHs. As shown in Fig. 5, more compounds with less nC (nC < 8) are present under the low RH experiment, also indicating that more SVOCs in the gas phase condense onto the particles.

The higher O:C ratio in the negative ion mode demonstrates that the compounds in the negative ion mode are much more oxygenated than those in the positive ion mode. As shown in Fig. 5, the peak intensities at high RH are much lower in the negative ion mode than in the positive mode, indicating that the decrease of the more oxygenated compounds accounts for
30 the larger fraction at high RH. These high O:C ratios cannot be explained by any of the formerly known oxidation pathways, except that the formation of HOMs from RO₂ autoxidation is taken into consideration (Crouse et al., 2013; Barsanti et al., 2017). To our knowledge, RH does not directly impact the formation of HOMs (Li et al., 2019). It is possible that HOMs undergo further particle-phase reactions as it has been suggested in a few studies (Bianchi et al., 2019) which may be influenced by RH, but this process need to be further investigated in the future studies. Moreover, the wall process of

the reactor enlarges the difference of SOA mass between low and high RH. The wall loss of some chemical species is faster at high RH, which leads to the reduction of SOA yield.

Response to Referee #4

We greatly appreciate the time and effort that referee 4 spent in reviewing our manuscript. The comments are really thoughtful and helpful to improve the quality of our paper. Referee 4 has provided both main comments and other specific comments. Below we make a point-by-point response to these comments. According to editor's requirement, the response to the referee 4 is structured in the following sequence: (1) comments from the referee in black color, (2) our response in blue color, and (3) our changes in the revised manuscript in red color.

The effect of relative humidity on yield and chemical composition of secondary organic aerosol originated from the photooxidation of *m*-xylene with OH radicals was investigated. Two analytical techniques were used to investigate the SOA chemical composition: Fourier transform infrared spectrometer (FTIR) for functional groups analysis and ultrahigh performance liquid chromatograph-electrospray ionization-high-resolution mass spectrometer (UPLC-ESI-HRMS) for structural elucidation. Two Relative humidity were investigated in this study. A chemical mechanism was proposed to account for the RH effect on SOA formation.

The experimental results show a significant yield increase as well as changes in chemical composition when the RH was increased from ~14% to ~75%. These results are consistent with most literature data either for the same system or for other aromatics (e.g. toluene). These data are important to atmospheric scientists interested in local/regional and global modeling because of the high-water content in the atmosphere. The role of water in atmospheric chemistry is still not well understood.

1. The authors investigated the effect of RH only at two points. I do feel that additional RH (for example at dry conditions <5%, ~30 and 45 %) will benefit the paper and the conclusion associated with the chemical composition changes as the RH changes.

Taking the reviewer's advice, we have added a few experiments at the RH values between 14% and 74%, as shown in Exps. 3-5 of Table 1. We have also replotted Fig. 1 for the addition of these three new experiments. The addition of these three experiments reconfirms the result of negative effect of RH on SOA formation. According to this comment and the comment 3 of referee 3, we have revised the Sec. 3.1. Please also see the reply of comment 3 of referee 3.

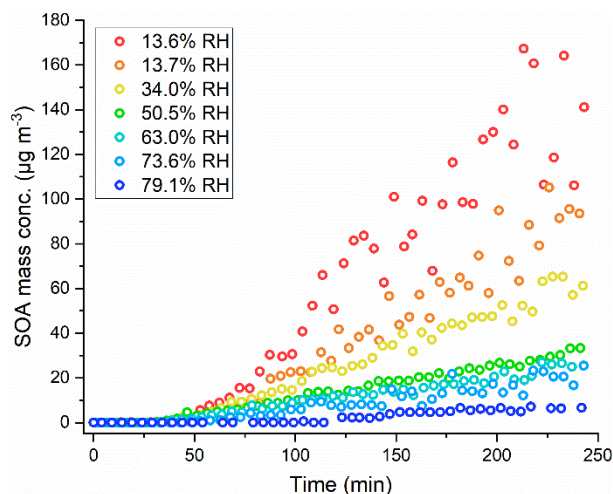
Table 1. Experimental conditions, SOA concentrations and yields at 4 h of experiments in *m*-xylene-OH oxidation system.

Exp. No.	$[m\text{-xylene}]_0$ ($\mu\text{g m}^{-3}$)	$[\text{H}_2\text{O}_2]_0^{\text{a}}$ (ppm)	RH (%)	T ($^{\circ}\text{C}$)	$[m\text{-xylene}]_{\text{reacted}}$ ($\mu\text{g m}^{-3}$)	$[\text{LWC}]_{4\text{h}}^{\text{b}}$ ($\mu\text{g m}^{-3}$)	$[\text{SOA}]_{4\text{h}}^{\text{b}}$ ($\mu\text{g m}^{-3}$)	SOA yield (%)
1	2287.9	20	13.6	25.9	1026.3	-	150.3 ± 15.0	14.6 ± 1.5

2	1855.5	20	13.7	25.3	682.0	-	95.5 ± 9.5	14.0 ± 1.4
3	2157.1	20	34.0	26.0	922.9	3.5 ± 0.3	61.1 ± 6.1	6.6 ± 0.7
4	2041.9	20	50.5	25.5	837.2	2.9 ± 0.3	33.3 ± 3.3	4.0 ± 0.4
5	2233.3	20	63.0	25.9	722.5	5.4 ± 0.5	25.0 ± 2.5	3.5 ± 0.3
6	2410.8	20	73.6	27.5	841.4	7.7 ± 0.8	21.0 ± 2.1	2.5 ± 0.2
7	2029.1	20	79.1	27.4	946.9	4.4 ± 0.4	7.5 ± 0.7	0.8 ± 0.1

^aCalculated using the density and mass concentration of injected H₂O₂ solution, and the volume of the reactor.

^bThe mass concentration at 4 h of reaction time with particle wall loss corrected.



5 **Figure 1.** SOA mass concentrations as a function of irradiation time (corrected by particle wall loss).

2. The volume of the reactor (although “smog chamber” was used: see my comment below) is 1-m³ and seems to me low. It is better to use the term Teflon bag instead of smog chamber (the experimental section is not clearly described). The use of small chamber volume is prone to high dilution rate when sampling is underway (SMPS, PILS...) and the authors did not correct the dilution in their yield calculations! The author needs to describe the experimental section more clearly: the sampling time (when the samples were taken either for the PILS or for FTIR, SMPS) should be provided. The authors mention only the samples were taken at the end of the experiment. What the end of experiment refers too here?

15 Taking the referee’s suggestion, we have changed the term smog chamber to the Teflon bag in the context of revised manuscript. Our Teflon bag is air-tight. When sampling is underway, there is no dilution. Indeed, the reactor volume is getting small when sampling but the change was not significant, as the total volume for sampling was only around 110 L during the reaction time, approximately 10% of the size of reactor. The durations of PILS for HRMS and DLPI for FTIR are 5 min and 15 min, respectively, and these two sampling were taken just after 4 h of reaction. Taking the referee’s advice, we

5 have added more content that the reactor is air-tight at the beginning of Sec. 2.1 and the sampling time of DLPI and PILS in the paragraphs 2 and 3 of the Sec. 2.2 in the revised manuscript. The experiments lasted for 4 h, so the end of experiment refers to 4 h of reaction from the start of the experiment, which has been addressed in the Sec. 2.1. In addition, we have added a sentence to state what is the end of experiment referred to in our study at the end of the Sec. 2.1 in the revised manuscript.

Experiments of *m*-xylene photooxidation were performed in a 1 m³ air-tight Teflon FEP film reactor...

10 The duration of DLPI for FTIR was 15 min, and this sampling was taken just after 4 h of each experiment.

The duration of PILS was 5 min, and this sampling was taken just after 4 h of each experiment.

Thus, the “end” of the experiment in this study refers to the experiment at 4 h of reaction time.

15 3. The yield was calculated by subtracting the LWC from the SOA mass. Two methods were used to measure (estimate) LWC at low and high RH. LWC measurements should be described in the manuscript clearly.

Taking the referee’s suggestion, we have rewritten the description of LWC measurement for clarification.

20 The size distribution and concentrations of particles were monitored with a scanning mobility particle sizer (SMPS, Model 3936, TSI, USA). The particle wall loss constant has been determined to be $3.0 \times 10^{-5} \text{ s}^{-1}$ and $6.0 \times 10^{-5} \text{ s}^{-1}$ at low RH and moist conditions, respectively. In experiments under moist conditions, particles measured by SMPS consisted of liquid water content (LWC) and SOA. In low RH experiments, as SOA hardly absorbs aerosol water, LWC can be negligible. Thus, the SOA mass can be directly measured by SMPS in low RH experiments. To obtain the SOA mass in high RH experiments,
25 LWC should be excluded from total particle mass. The method for the measurement of LWC has been already described in the previous study (Jia and Xu, 2018), so here a brief introduction is only provided. During each high RH experiment, the SMPS measured the humid particles. After 4 h from the start of oxidation reaction in each high RH experiment, the SMPS was modified to the dry mode. In the dry mode, a Nafion dryer (Perma Pure MD-700-12F-3) was added to the sampling flow and a Nafion dryer (Perma Pure PD-200T-24MPS) was added to the sheath flow. After the modification of SMPS, the humid
30 air in SMPS was quickly replaced by dry air through venting the sheath air at 5 L min^{-1} , so that the RH in the sheath air can decrease to 7%. Then, SMPS at this dry mode measured dry particle concentrations as the RH in the sample air decreased to 10% at this time. The LWC was determined by the difference of the particle mass concentrations before and after the SMPS modification to the dry mode.

4. The use of the term “HOM” is confusing to me. It was used in section 3.4 2nd paragraph to describe products associated with OH abstraction and addition to *m*-xylene. I feel that compounds mentioned in the first paragraph of this section (3.4) should also be called “HOM”. The authors should define exactly the term “HOM” in this paper.

5 Taking the reviewer’s advice and the comment 15 of Referee 3, we have revised the content in Sec. 3.4. The HOM is referred to the highly oxygenated organic molecules that have been provided in the revised Sec. 3.4.

5. Deducing structures from HRMS mass spectra only can be misleading due to issues that can arise from LCMS instruments (e.g. solvents, unpredictable clusters formations etc.). The authors should be careful reporting these data (structures) without the benefit of reporting and interpreting MS/MS spectra associated with each compound tentatively identified in this study (see Table 3). The paper lack of providing and interpreting MS/MS spectra that could make the identification straightforward and robust. For example, MS/MS of reaction products (or selected products) in Scheme 1 identified by HRMS should be presented in the manuscript or in supplementary information.

15 Taking the referee’s suggestion, we have added the MS² spectra of compounds mentioned in Table 3 in the supporting information, as can be seen in the reply of Comment 10 of referee 3. We agree with the referee that the structures in Scheme 1 should be carefully assigned. So we have deleted some assignments in the Scheme 1 in the revised manuscript.

6. In the abstract and in page 5 (lines 3-5), the authors report using the MCM mechanism as a tool to explain the RH effect and analyse products measured by HRMS. The following sentence is confusing to me “The reaction pathways and products of *m*-xylene-OH photooxidation in Master Chemical Mechanism (MCM v3.3.1, the website at <http://mcm.leeds.ac.uk/MCM>; last accessed October 16, 2017) was used for analysis of the products measured by HRMS (Jenkin et al., 2003; Jia and Xu, 2014).” Throughout the manuscript, the MCM mechanism was not used and these statements are not consistent with the data provided in this paper. Although, adding a section to the manuscript focusing on linking products observed in this work with the MCM mechanism will be beneficial and make the paper stronger.

In the manuscript, we listed a Table 3 to show the peaks that were measured by HRMS, whose structures can be proposed according to the gas-phase chemical mechanism of *m*-xylene-OH photooxidation included in MCM. Also, the content focusing on the linking products observed in HRMS with the MCM mechanism is already in the second paragraph of Sec. 3.3.

Other comments

1. Abstract. The sentence “The relative increase of C-O-C at high RH from the FTIR analysis of functional groups indicates that the oligomers from carbonyl compounds cannot well explain the suppression of SOA yield.” Is not consistent with the data shown in Figure 2. The absorptions at 1180 cm⁻¹ associated to C-O-C are higher under high RH than low RH?? Comments from the authors.

5

Yes, it is consistent with data in Fig. 2. In fact, the absorptions at 1180 cm⁻¹ associated to C-O-C are lower under high RH than low RH as shown in Fig. 2. However, the ratio of the SOA mass collected on disk at high RH to that at low RH is 0.29 while the ratio of peak intensities at high RH to that at low RH is 0.48, so we used the “relative increase” of C-O-C in the Abstract. It means under different RH conditions the proportion of oligomers is different. For clarification we have rephased this sentence in the Abstract.

10

The FTIR analysis shows that the proportion of oligomers with C-O-C groups from carbonyl compounds in SOA at high RH is higher than that at low RH, but further information cannot be provided by the FTIR results to well explain the negative RH effect on SOA formation.

15

2. The experimental section should be described clearly. I’m confused with the sentence describing the chamber “...Teflon FEP film reactor (...) in an indoor smog chamber”. What the authors refers to indoor smog chamber in this contest? Are all reactants were introduced initially and then the light was turned on and the reaction starts. Please explain how the experiment was conducted? How H₂O₂ was evaporated to the reactor? Initial H₂O₂ concentrations should be provided in table 1. The experimental section should be described then readers can clearly understand how the experiment was conducted?

20

The indoor smog chamber we refer to is relative to the outdoor smog chamber, which indicates whole experiment system, including Teflon bag, light source, etc. In this study, all reactants were introduced initially and then the light was turned on and the reaction starts. Taking the referee’s suggestion, we have added a sentence for clear description of the experiment and rewritten the sentences about the description of experimental procedure in the last paragraph of Sec. 2.1 in the revised manuscript. Also, we have added the H₂O₂ concentrations in Table 1 which can be seen in the reply of comment 1.

25

Hydrogen peroxide was introduced into the reactor along with the zero air flow over a period of 30 min via an injection of H₂O₂ solution (30 wt %) into a three-way tube using a syringe to the desired concentration of 20 ppm...All reactants were introduced initially and then the light was turned on and the reaction starts...

30

3. Page 4, line 13. How LWC was measured at high RH? This is very important since yield are derived from (total aerosol mass – LWC)? Why the method used for low RH was not used for high RH to deduct LWC?

Please see the reply of the major comment 3 above which is similar with this comment.

4. Is the density the same at high and low RH conditions?

5 Yes, the density for SOA is the same for high and low RH conditions, but it is different for particles. A value of 1.4 g cm^{-3} for SOA is used in our work. Song et al. (2007) investigated the density of SOA formed from the oxidation of *m*-xylene under dried conditions in the absence of NO_x and gave the density of 1.4 g cm^{-3} .

5. Page 4, lines 15-16. This sentence is not clear. Are the authors mean: “The chemical composition of SOA originated from *m*-xylene-OH irradiation was investigated using Fourier transform infrared spectrometer (FTIR).” instead of “For the analysis of functional groups of the chemical composition in SOA from *m*-xylene-OH irradiation, the SOA samples were collected and determined by FTIR (Fourier transform infrared spectrometer).”

Taking the referee’s suggestion, we have rewritten the sentence in the revised manuscript.

15

The chemical composition of SOA originated from *m*-xylene-OH irradiation was investigated using Fourier transform infrared spectrometer (FTIR), which can provide the information of functional groups.

6. Page 4, line 17 and Table 1. What the end of the experiment refers too? Please state the exact time when samples were taken and for how long as well as the reaction time for data reported in Table 1. Are the disks were analysed directly after the sampling?

The end of the experiment refers to 4 h after the light was turned on. Sampling was made just after the end of experiments. The reaction time for data reported in Table 1 was 4 h. The disk was analysed directly after sampling. Taking the referee’s advice, the above content has been added or rewritten in the manuscript for clear description, which can be seen in the reply of the major comment 2.

7. Table 1 should incorporate the LWC and reacted *m*-xylene and may be *m*-xylene if it was measure at several reaction time? Is all *m*-xylene was reacted at the time when samples were taken? The authors may show in Figure 1 the sampling time associated with each RH!

Taking the referee’s suggestion, we have added the LWC and reacted *m*-xylene in Table 1, which can be seen in the reply of Comment 1. The *m*-xylene was measured at several reaction time points as shown in Fig. S1 in the supporting information. When the samples for particle analysis were taken, the *m*-xylene was not all reacted. As shown in Fig. S1, ~40% *m*-xylene

was reacted for each experiment. These two samples used for HRMS and for FTIR were taken just after 4 h of reaction, and the sampling durations of PILS for HRMS and DLPI for FTIR were 5 min and 15 min, respectively, which has been added in the Sec. 2.2 in the revised manuscript and can be seen in the reply of the major comment 2.

5 8. Are the SOA masses reported in Table 1 includes LWC?

The SOA masses reported in Table 1 do not include LWC.

9. Figure 1. Is the temperature being constant throughout the experiment? In general, the initial RH should decrease as the
10 reaction progress and fluctuation of the temperature should be observed as the light is turned on. The RH provided in Table 1
is for the “end” of the experiment or the initial RH? I would prefer to see RH, temperature also included in Figure 1 as the
reaction progresses. If the RH provided in figure 1 and Table 1 are at the “end” of the experiment (again is confusing to use
the end of the experiment) then what was the initial RH and temperature at t=0 min? The term “end“ is misleading and prefer
to state the exact time.

15

Throughout the experiment a temperature probe was installed outside and close to the Teflon bag to monitor the temperature
in real-time. At t = 0 and t = 4 h of an experiment a portable hygrometer with higher accuracy was used to obtain the
temperature and RH inside the Teflon bag which is given in Table 1. Before lights were turned on, the temperature was
controlled using air-conditioners to be 26°C measured by the temperature probe. After lights were turned on, we adjusted the
20 setting temperature of the air-conditioners to maintain the temperature probe value to be 26°C. Indeed, there was a slight
fluctuation of temperature at the first half hour. Then, the temperature was steady within a fluctuation of 0.5°C obtained by
the temperature probe. As the temperature and RH were steady during most of the reaction time, we used the temperature
and RH measured by the portable hygrometer to present, as shown in Table 1. The temperature and RH were not
continuously recorded throughout the experiment, so we cannot provide the results with RH and temperature in Fig. 1 as the
25 reaction progressed. Taking the referee’s suggestion, we have changed the term “end” to the exact time in Table 1 and the
context in the revised manuscript.

10. Does Figure 5 is necessary? I suggest reporting MS/MS spectra instead of this figure. I feel Figure 4 provides enough
information?

30

Taking the referee’s suggestion, we have deleted Fig. 5. The MS/MS spectra have been added as Fig. S3 in the supporting
information based on the comment 10 from referee 3.

Secondary organic aerosol formation from OH-initiated oxidation of *m*-xylene: effects of relative humidity on yield and chemical composition

Qun Zhang^{1,2}, Yongfu Xu^{1,2,*}, Long Jia^{1,2}

5 ¹State Key Laboratory of Atmospheric Boundary Layer Physics and Atmospheric Chemistry, Institute of Atmospheric Physics, Chinese Academy of Sciences, Beijing 100029, China,

²Department of Atmospheric Chemistry and Environmental Sciences, College of Earth Sciences, University of Chinese Academy of Sciences, Beijing 100049, China

Correspondence to: Yongfu Xu (xyf@mail.iap.ac.cn)

10 **Abstract.** The effect of relative humidity (RH) on the secondary organic aerosol (SOA) formation from the photooxidation of *m*-xylene initiated by OH radicals in the absence of seed particles was investigated in a Teflon reactor. The SOA yields were determined based on the particle mass concentrations measured with a scanning mobility particle sizer (SMPS) and reacted *m*-xylene concentrations measured with a gas chromatograph-mass spectrometer (GC-MS). The SOA components were analysed using Fourier transform infrared spectrometer (FTIR) and ultrahigh performance liquid chromatograph-

15 electrospray ionization-high-resolution mass spectrometer (UPLC-ESI-HRMS). A significant decrease was observed in SOA mass concentration and yield variation with the increasing RH conditions. The SOA yield is 14.6% and 0.8% at low RH (13.6%) and high RH (79.1%), respectively, with the difference being over an order of magnitude. The chemical mechanism for explaining the RH effects on SOA formation from *m*-xylene-OH system is proposed based on the analysis of both FTIR and HRMS measurements, and the Master Chemical Mechanism (MCM) prediction is used as the assistant. The FTIR

20 analysis shows that the proportion of oligomers with C-O-C groups from carbonyl compounds in SOA at high RH is higher than that at low RH, but further information cannot be provided by the FTIR results to well explain the negative RH effect on SOA formation. In the HRMS spectra, it is found that C₂H₂O is one of the most frequent mass difference at low and high RHs, that the compounds with lower carbon number in the formula at low RH account for a larger proportion than those at high RH, and that the compounds at high RH have higher O:C ratios than those at low RH. The HRMS results suggest that

25 the RH may suppress the oligomerization where water is involved as a by-product and may influence the further particle-phase reaction of high oxygenated organic molecules (HOMs) formed in the gas phase. In addition to the chemical processes, the negative RH effect on SOA formation is enlarged based on the gas to particle partitioning rule.

1 Introduction

Secondary organic aerosol (SOA) is a significant component of atmospheric fine particulate matter in the troposphere

30 (Hallquist et al., 2009; Spracklen et al., 2011; Huang et al., 2014), leading to serious concerns as it has a significant influence on the air quality, oxidative capacity of the troposphere, global climate change and human health (Jacobson et al., 2000;

Hansen and Sato, 2001; Kanakidou et al., 2005; Zhang et al., 2014). In a previous study from a global model simulation, it has been found that SOA represents a large fraction, approximately 80% of the total organic aerosol sources (Spracklen et al., 2011).

5 The formation of SOA in the atmosphere is principally via the oxidation of volatile organic compounds (VOCs) by common atmospheric oxidants such as O₃, OH and NO₃ radicals (Seinfeld and Pandis, 2016). Aromatic compounds mainly from anthropogenic source, including solvent usage, oil-fired vehicles and industrial emissions, contribute 20-30% to the total VOCs in urban atmosphere, which play a significant role in the formation of ozone and SOA in the urban troposphere (Forstner et al., 1997; Odum et al., 1997; Calvert et al., 2002; Bloss et al., 2005; Offenberg et al., 2007; Ding et al., 2012; Zhao et al., 2017). Amongst aromatics, *m*-xylene is significant, of which mean concentration together with *p*-xylene in
10 daytime was determined up to 140.8 μg m⁻³ in atmosphere of urban areas in developing countries (Khoder, 2007).

The oxidation of aromatics in the troposphere is mainly initiated through OH radicals, which is affected by many chemical and physical factors. The concentrations of oxidant species, VOCs and NO_x concentrations, as well as the ratio of VOCs to NO_x (Ge et al., 2017b) determine the main chemical mechanism. Light intensity (Warren et al., 2008), temperature (Qi et al., 2010) and relative humidity (RH) are the most significant physical parameters that affect the chemical process. RH governs
15 the water concentration in the gas phase and the liquid water content (LWC) in the particle phase. Water plays a significant role that can serve as reactant, product and solvent to directly participate in chemistry (Finlayson-Pitts and Pitts Jr., 2000) and indirectly affect the reaction environment such as acidity of particles (Jang et al., 2002). **Acid-catalysis of heterogeneous reactions of atmospheric organic carbonyl species in particle phase can lead to a large increase of SOA mass, while this process can be suppressed by the lower acidity at high RH (Czoschke et al., 2003). In addition, RH can change the viscosity of SOA and further affect the chemical processed of SOA formation (Kidd et al., 2014; Liu et al., 2017).**
20

Investigations of RH effects on aromatics SOA have been conducted in many previous works. In the presence of NO_x, it was observed that RH significantly enhanced the yield of SOA from benzene, toluene, ethylbenzene and xylenes photooxidation, which was explained by a higher formation of HONO, particle water, aqueous radical reactions and the hydration from glyoxal (Healy et al., 2009; Kamens et al., 2011; Zhou et al., 2011; Jia and Xu, 2014, 2018; Wang et al., 2016). Meanwhile,
25 under low NO_x condition that no NO_x were introduced artificially and photolysis of H₂O₂ was as an OH radical source, it has been observed that deliquesced seed contributed to the enhancement of SOA yield from toluene (Faust et al., 2017; Liu et al., 2018). However, under low NO_x level, it has been found that, in the study on toluene SOA formation, moderate RH level (48%) leads to a lower SOA yield than low RH level (17-18%) (Cao and Jang, 2010). In a most recent study on SOA formation of toluene (Hinks et al., 2018), high RH led to a much lower SOA yield than low RH under low NO_x level, which
30 is attributed to condensation reactions that remove water, leading to the less oligomerization at high RH. In a study on chemical oxidative potential of SOA (Tuet et al., 2017) under low NO_x conditions, it was observed that the mass concentration of SOA from *m*-xylene irradiation under the dry condition was much larger than that under the humid condition, whereas the study did not focus on the RH effect on *m*-xylene SOA formation. These demonstrate that the RH

effects on aromatics SOA yields, especially *m*-xylene, have not been fully understood and the RH effects are controversial under various NO_x levels and seed particle conditions.

Chemical components of SOA are important, on which climate- and health-relevant properties of particles are dependent. Chemical compositions of SOA from aromatics-NO_x photooxidation have been investigated by GC/MS analysis (Forstner et al., 1997). Nevertheless, this study was only performed at 15-25% RH and high temperature at GC injection ports can easily decompose some low-volatile substances in SOA. FTIR was also used to study chemical compositions of SOA from aromatics-NO_x photooxidation under different RH conditions, in which the information of functional groups in SOA was provided (Jia and Xu, 2014, 2018). **In these studies, O-H, C=O, C-O, and C-OH were found to be the main functional groups, intensities of which largely increased with increasing RH. Compounds in SOA with the O-H group mainly contributed to the** **increase of SOA, such as polyalcohols formed from aqueous reactions.** The recent study on SOA components from toluene-OH system under both dry and humid conditions were analysed via HRMS (Hinks et al., 2018). Although the information of chemical compositions in SOA has been given, the analysis and the mechanism of RH effects still need to be further studied.

RH effects on SOA formation from *m*-xylene under low NO_x condition have not been studied well. In the present study, we present the results from the experiments about the SOA formation from the OH-initiated oxidation of *m*-xylene in the absence of seed particles in a **Teflon bag. The SOA yields at different RHs and the chemical components under both low and high RH conditions will be reported.** The underlying mechanism of SOA formation for these different conditions will be also discussed.

2 Experimental materials and methods

2.1 Equipment and reagents

Experiments of *m*-xylene photooxidation were performed in a 1 m³ **air-tight** Teflon FEP film reactor (DuPont 500A, USA), which is similar to our previous works (Jia and Xu, 2014, 2016, 2018; Ge et al., 2016, 2017a, b, c). So only a brief introduction is presented here. A light source was provided by 96 lamps (F40BLB, GE; UVA-340, Q-Lab, USA) **surrounding the Teflon bag** to simulate the UV band of solar spectrum in the troposphere. The NO₂ photolysis rate was determined to be 0.23 min⁻¹, which was used to reflect the light intensity in the reactor. To remove the electric charge on the surface of the FEP reactor, two ionizing air blowers were equipped **outside the Teflon bag** and were used throughout each experiment.

The background gas was zero air, which was generated from Zero Air Supply and CO Reactor (Model 111 and 1150, Thermo Scientific, USA) and further purified by hydrocarbon traps (BHT-4, Agilent, USA). **The humid zero air** was obtained by bubbling dry zero air through ultrapure water (Milli Q, 18MU, Millipore Ltd., USA). **To obtain the different desired RH in the reactor, the different ratio dry and humid zero air was mixed.** The RH and temperature in the reactor were measured by a hygrometer (Model 645, Testo AG, Germany).

Throughout each experiment, the background NO_x concentration in the reactor was lower than 1 ppb and OH radicals were provided from H₂O₂ photolysis. Hydrogen peroxide was introduced into the reactor along with the zero air flow over a period of 30 min via an injection of H₂O₂ solution (30 wt %) into a three-way tube using a syringe to the desired concentration of 20 ppm. Though the H₂O₂ level was not measured, it was estimated through the measured volume of H₂O₂ solution evaporated. *m*-Xylene (99%, Alfa Aesar) was introduced to the reactor subsequently using the same approach. No seed particles were introduced artificially. All reactants were introduced initially and then the light was turned on and the reaction starts. The experiments were conducted for 4 h. Thus, the “end” of the experiment in this study refers to the experiment at 4 h of reaction time.

2.2 Monitoring and analysis

The concentration of *m*-xylene in the reactor was measured with a gas chromatograph-mass spectrometer (GC-MS, Model 7890A GC and Model 5975C mass selective detector, Agilent, USA), which was equipped with a thermal desorber (Master TD, Dani, Italy). The size distribution and concentrations of particles were monitored with a scanning mobility particle sizer (SMPS, Model 3936, TSI, USA). The particle wall loss constant has been determined to be $3.0 \times 10^{-5} \text{ s}^{-1}$ and $6.0 \times 10^{-5} \text{ s}^{-1}$ at low RH and moist conditions, respectively. In experiments under moist conditions, particles measured by SMPS consisted of liquid water content (LWC) and SOA. In low RH experiments, as SOA hardly absorbs aerosol water, LWC can be negligible. Thus, the SOA mass can be directly measured by SMPS in low RH experiments. To obtain the SOA mass in high RH experiments, LWC should be excluded from total particle mass. The method for the measurement of LWC has been already described in the previous study (Jia and Xu, 2018), so here a brief introduction is only provided. During each high RH experiment, the SMPS measured the humid particles. After 4 h from the start of oxidation reaction in each high RH experiment, the SMPS was modified to the dry mode. In the dry mode, a Nafion dryer (Perma Pure MD-700-12F-3) was added to the sampling flow and a Nafion dryer (Perma Pure PD-200T-24MPS) was added to the sheath flow. After the modification of SMPS, the humid air in SMPS was quickly replaced by dry air through venting the sheath air at 5 L min^{-1} , so that the RH in the sheath air can decrease to 7 %. Then, SMPS at this dry mode measured dry particle concentrations as the RH in the sample air decreased to 10 % at this time. The LWC was determined by the difference of the particle mass concentrations before and after the SMPS modification to the dry mode.

The chemical composition of SOA originated from *m*-xylene-OH irradiation was investigated using Fourier transform infrared spectrometer (FTIR), which can provide the information of functional groups. The particles were collected on a ZnSe disk using a Dekati low-pressure impactor (DLPI, Dekati Ltd., Finland) at the end of each experiment (Ge et al., 2016; Jia and Xu, 2016). The duration of DLPI for FTIR was 15 min, and this sampling was taken just after 4 h of each experiment. Then, the ZnSe disk was directly put in a FTIR (Nicolet iS10, Thermos Fisher, USA) for the measurement of functional groups of the chemical composition in SOA samples.

To obtain the detailed information of chemical composition, SOA particles were sampled using the Particle into Liquid Sampler (PILS, model 4001, BMI, USA). The PILS samples water-soluble species in particles. As the SOA compositions are

almost all water-soluble species, it is reasonable and reliable to use PILS to sample SOA for analysis of chemical composition. The flow rate of sample gas was around 11 L min⁻¹, and the output flow rate of liquid sample was 0.05 mL min⁻¹. Two denuders were used to remove the VOCs and acids in the sample gas. SOA liquid samples collected by PILS were finally transferred into vials for subsequent analysis of mass spectrometry. The duration of PILS was 5 min, and this sampling was taken just after 4 h of each experiment. Operatively, the blank measurements were obtained by replacing the sample gas with zero air collected in vials. It is well known that the PILS samples water-soluble species in the SOA with high efficiency. In addition, it is reported that the PILS can also samples slightly water-soluble organic compounds with average O:C ratios higher than 0.26 instead of the total SOA composition and the collection efficiency could exceed 0.6 (Zhang et al., 2016). Thus, the PILS can sample the overwhelming majority of the SOA system in our study, though PILS cannot sample water-insoluble species in the SOA.

The accurate mass of organic compounds in SOA and their MS/MS fragmentations were measured by the ultrahigh performance liquid chromatograph (UPLC, Ultimate 3000, Thermo Scientific, USA)-heated-electrospray ionization-high-resolution orbitrap mass spectrometer (HESI-HRMS, Q Exactive, Thermo Scientific, USA). Methanol (Optima™ LC/MS Grade, Fisher Chemical, USA) was used as the eluent in UPLC system. The elution flow rate was 0.2 mL min⁻¹, and the overall run time was 5 minutes. The injection volume was 20 μL. In this study, the UPLC was only used as the injection system of HRMS. The acquired mass spectrum of SOA was in the range of 80-1000 Da. The HESI source was conducted in both positive and negative ion modes using the optimum method for characterization of organic compounds. We used the Thermo Scientific Xcalibur software (Thermo Fisher Scientific Inc., USA) to analyse the data from HRMS. To calculate the elemental compositions of compounds, the accurate mass measurements were used. For further analysis of the data from the second stage of data-dependent mass spectrometry (ddMS²), the Mass Frontier program (Version 7.0, Thermo Fisher Scientific Inc., USA) was used in order to simulate breaking the ions into fragments for comparison with the measured fragments to assist in identifying the structures. The reaction pathways and products of *m*-xylene-OH photooxidation in Master Chemical Mechanism (MCM v3.3.1, the website at <http://mcm.leeds.ac.uk/MCM>; last accessed October 16, 2017) was used for analysis of the products measured by HRMS (Jenkin et al., 2003; Jia and Xu, 2014).

3. Results and discussion

3.1 RH effects on SOA yields

Seven experiments were conducted. The initial conditions, the LWC, SOA concentrations, yields and reacted *m*-xylene at the end of each experiment in *m*-xylene-H₂O₂ photooxidation system are summarized in Table 1. Exps. 1 and 2 were conducted in dry zero air, which are defined as the low RH experiments. Exps. 6 and 7 were conducted in humid zero air, which are defined as the high RH experiments. Exps. 3-5 were conducted in the mixed air of dry and humid zero air, which are defined as the intermediate RH experiments. Under intermediate and high RH conditions, LWC accounts for a certain proportion of particles (Jia and Xu, 2018). To obtain the time evolution of SOA concentrations, the LWC has to be subtracted during the

whole photooxidation period. Since LWC was only measured at the end of the reaction, the volume growth factor (VGF) was used to estimate the contribution of LWC in particles, which was defined as the ratio of the humid particle volume to the dry particle volume (Engelhart et al., 2011). It was assumed that the VGF did not change during the whole photooxidation period. Thus, the LWC can be obtained by VGF. As shown in Fig. 1, the wall-loss-corrected SOA mass concentrations are plotted as a function of photooxidation reaction time for *m*-xylene-OH systems at different RHs. The removal of aerosol water during the LWC measurement may cause the dissolved species that are probably volatile/ semi-volatile compounds to evaporate back into the gas phase. Glyoxal is a typical semi-volatile compound with high Henry's law constant, which is involved in SOA formation in *m*-xylene-OH system of our study. The Henry's law constant of glyoxal in pure water is as high as $4.19 \times 10^5 \text{ M atm}^{-1}$ at 298 K (Ip et al., 2009). Only one in ten thousand of glyoxal can dissolve in the LWC whose concentration was obtained in our study. Thus, SOA concentrations for intermediate and high RH conditions were slightly underestimated, but the underestimation is extremely low and can be negligible.

It can be clearly observed that there is a large difference in the maximum mass concentration between low and high RHs. The maximum mass concentrations fitted are 150.3 and 95.5 $\mu\text{g m}^{-3}$ at low RHs, whereas they are 21.0 and 7.5 $\mu\text{g m}^{-3}$ at high RHs, with the largest difference being over ten times. The RH effect was reproducible when the initial *m*-xylene concentration was changed under similar conditions. To obtain the particle mass concentrations and SOA yield, an SOA density of 1.4 g cm^{-3} was used (Song et al., 2007). The fairly large scatter in the mass concentrations of SOA in Fig. 1 was observed, which mainly results from the uncertainty of SOA measurement by SMPS instrument. The interval of SOA data sampled by SMPS was 5 minutes, for which the sampling frequency was relatively low. Technically, according to the instruction manual of the CPC (Model 3776), the particle concentration accuracy is $\pm 10\%$ at $< 3 \times 10^5 \text{ particles cm}^{-3}$. The number concentrations at the end of each experiment in this study were below $5 \times 10^3 \text{ particles cm}^{-3}$, so in this study the particle concentration error caused by CPC alone was $\pm 10\%$. In addition, size-dependent aerosol charging efficiency uncertainties and CPC sampling flow rate variability also dominate the SMPS measurement uncertainty. The combination of various uncertainties, including SMPS measurement, sampling and even conversion of mass concentration from number concentration leads to the fairly large scatter in Fig. 1.

We used the definition of the ratio of the SOA mass to the consumed *m*-xylene mass to calculate the SOA yield at the end of each experiment. As summarized in Table 1, the SOA yields at low RH are 14.0-14.6%, while those at high RH are only around 0.8-2.5%. Both mass concentrations and SOA yields at low RH are an order of magnitude larger than those at high RH. Though temperatures at high RH are slightly higher than those at low RH as shown in Table 1, which can lead to a higher SOA yield, the difference of temperatures between low and high RH conditions is lower than two degree, which cannot lead to a significantly different SOA yield to affect the result (Qi et al., 2010).

Seed aerosols were not artificially introduced throughout all the experiments, which could lead to the underestimation of SOA, as SOA-forming vapours partly condense to the reactor walls instead of particles (Matsunaga and Ziemann, 2010; Zhang et al., 2014). The extent to which vapor wall deposition affects SOA mass yields depends on the specific parent hydrocarbon system (Zhang et al., 2014; Zhang et al., 2015; Nah et al., 2016; Nah et al., 2017). Zhang et al (2014) have

estimated two *m*-xylene systems under low NO_x conditions and concluded that SOA mass yields were underestimated by factors of 1.8 (Ng et al., 2007) and 1.6 (Loza et al., 2012) under low RH conditions. In addition, the excess use of H₂O₂ can lead to an excess OH radicals, leading to a less underestimation of SOA formation as the losses of SOA-forming vapours can be mitigated via the use of excess oxidant concentrations (Nah et al., 2016). Thus, the underestimation of SOA formation can be limited. In fact, the wall loss of *m*-xylene was not taken into consideration of calculation of mass yields, which generally overestimates the mass yields.

The wall loss of chemical species that is sensitive to humidity may affect the RH effect on SOA yields, as the reduction of SOA yields at the high humidity may be due to the chemical loss to the wet reactor wall. To estimate the extent of how much the wall loss of chemical species affects the SOA formation at different RHs, we take glyoxal and acetone as reference compounds. Glyoxal, a typical compound that can form SOA, can easily dissolve in the aqueous phase due to the large Henry's law constant of $4.19 \times 10^5 \text{ M atm}^{-1}$ at 298 K (Ip et al., 2009), very sensitive to humidity. Loza et al. (2010) found that the wall loss of glyoxal was minimal at 5% RH, with $k_w = 9.6 \times 10^{-7} \text{ s}^{-1}$, whereas k_w was $4.7 \times 10^{-5} \text{ s}^{-1}$ at 61% RH. We assume that k_w linearly increases with RH, and the k_w value is estimated to be $6.1 \times 10^{-5} \text{ s}^{-1}$ at 80% and 7.4×10^{-6} at 13% RH, with the difference being 8.2 times. According to the wall loss of glyoxal, glyoxal only decreased by 10% at the end of our experiment at low RH, while glyoxal decreased by 59% at high RH. Acetone can hardly dissolve in the aqueous phase due to the small Henry's law constant of 29 M atm^{-1} (Poulain et al., 2010), which is 4 orders of magnitude less than that of glyoxal. Ge et al. (2017) obtained that the wall loss of acetone was $5.0 \times 10^{-6} \text{ s}^{-1}$ at 87% RH and $3.3 \times 10^{-6} \text{ s}^{-1}$ at 5% RH, with a factor of 1.5. The difference of wall loss between glyoxal and acetone at low RH is about 2 times, while it becomes about 12 times at high RH. Thus, it can be considered that the wall loss among different species at low RH is less affected by the Henry's law constant, but it is greatly affected at high RH. In our study glycolaldehyde (See the Sec. 3.4) is proposed to be an important SOA precursor that can form a large fraction of oligomers in our experiments, but the wall loss of glycolaldehyde is not available. The Henry's law constant of glycolaldehyde was obtained to be $4.14 \times 10^4 \text{ M atm}^{-1}$ (Betterson and Hoffmann, 1988), an order of magnitude lower than glyoxal, indicating that glycolaldehyde is less sensitive to humidity than glyoxal but much more sensitive to humidity than acetone. Based on the data of these two reference species, the wall loss of glycolaldehyde at low RH is taken to be $5 \times 10^{-6} \text{ s}^{-1}$, and the difference in wall loss between high and low RHs is about 6 times. Then, the wall loss of glycolaldehyde at high RH can be $3 \times 10^{-5} \text{ s}^{-1}$. Then, it is estimated that glycolaldehyde would decrease by 7% at low RH and by 35% at high RH at the end of our experiment, respectively. This means that SOA yield would be underestimated by 35% at high RH and by 7% at low RH if glycolaldehyde lost to the wall was completely transformed to SOA. If this wall effect of SOA precursors was taken into consideration, the SOA yields at high (Exp. 6) and low (Exp. 2) RHs would be 3.4% and 15.1%, respectively. Alternatively, the SOA yield at high RH was underestimated to be 42% relative to that at low RH. Even the sensitivity of the wall loss to RH was taken to be 8 times, the SOA yield at high RH would be underestimated to be 62% compared to that at low RH. In fact, there were many different SOA precursors from the *m*-xylene oxidation system that probably have much smaller Henry's law constant relative to that

of glycolaldehyde. Thus, it is concluded that the RH effect on SOA formation from *m*-xylene photooxidation by H₂O₂ is negative.

For comparison and discussion of the results of SOA formation with other previous studies, Fig. 2 was plotted to show the SOA yields as a function of RH for the different aromatic (toluene and *m*-xylene) oxidation under low NO_x conditions with the photolysis of H₂O₂ as the OH source. In Fig. 2, the hollow circles represent that no seed particles were introduced and the circles with a cross represent that seed particles were introduced, and the size of markers indicates the magnitude of amount of reacted VOC. In the most recent study on toluene SOA formation conducted without seed particles (Hinks et al., 2018), the SOA yield at low NO_x level was 15% under dry conditions (< 2% RH) and 1.9% under humid conditions (89% RH), with the ratio of two yields between dry and humid conditions being over 7.5. The toluene SOA produced under high RH conditions were significantly suppressed, in which the tendency of RH effects on SOA yield was very similar with our study, though the difference of SOA yield in the range of low and high RH conditions in Hinks et al (2018) was slightly smaller than that in this study. The small difference of RH effects between Hinks et al. and our study is likely associated with the difference in experimental conditions, including RHs, initial and reacted VOCs and H₂O₂ concentrations, in addition to different species. This comparison demonstrates that different species of toluene and *m*-xylene of aromatics pose very similar RH effects under low-NO_x conditions. Hinks et al. attributed the suppression of SOA yields by elevated RH to the lower level of oligomers generated by condensation reactions and the reduced mass loading at high RH. In a study on an SOA model for toluene oxidation, the negative RH effect on SOA formation was also found in the presence of seed particles (Cao and Jang, 2010). In their study, the SOA yield at low NO_x level was 28-30% under low RH conditions (17-18% RH) and 20-25% under moderate RH conditions (48% RH) (Cao and Jang, 2010), but they did not focus on the RH effect to give an explanation. Furthermore, their RH only changed from 17% to 48%, the reacted parent VOC was smaller and the seed particles were present, so the RH effect on SOA yields was not as significant as those in Hinks et al and our study. Ng et al. have investigated the yields of SOA formed from *m*-xylene-OH system at low RH (4-6%) under low NO_x conditions (Ng et al., 2007). They obtained that the SOA yields were in the range of 35.2-40.4% in the presence of seed particles. The SOA yields were larger than those of our study, as they conducted the experiments under different irradiation time and with inorganic seed particles. These seed particles can provide not only surface for chemical reactions, but also acidic and aqueous environments that can promote the SOA formation (Jang et al., 2002; Liu et al., 2018; Faust et al., 2017). The reacted concentration of parent VOC was close between Cao and Jang and Ng et al. though the species were different. The results from these two studies can be considered together, since their experiments all had seed particles. As shown in Fig. 2, the obviously negative RH effect on SOA yields can be found. In addition to these three previous studies shown in Fig. 2, a study on chemical oxidative potential of SOA (Tuet et al., 2017) found that the concentration of SOA from *m*-xylene irradiation at low NO_x level under dry condition was much larger than that under humid condition (89.3 μg m⁻³ at < 5% RH and 13.9 μg m⁻³ at 45% RH), but they did not calculate the *m*-xylene SOA yields or give an explanation for the RH effect.

3.2 RH effects on functional groups of SOA

Figure 2 shows the FTIR spectra of particles from the photooxidation of *m*-xylene-OH experiments under both low (Exp. 2) and high (Exp. 6) RH conditions. The DLPI sample flow rate was 10 L min⁻¹, and the sampling duration was 15 min. We used same sampling flow rate and duration for both RH conditions. DLPI has 13 stages, and it can collect particles in the size range of 30 nm - 10 μm. When we sampled using DLPI, the four plates for stages 4-7 were removed, so that particles in the range of 108-650 nm were collected on the third plate. As shown in Fig. S2 in the supplementary information, the particles in the range of 108-650 nm can represent the total SOA from *m*-xylene oxidation in this study. The mean collection efficiency of the DLPI was 83% for stages 4-7 (Durand et al., 2014). Thus, the SOA mass collected on the ZnSe window was 10.3 and 3.0 μg at low RH (Exp. 2) and high RH (Exp. 6), based on the SMPS measurement and the DLPI collection efficiency. As shown in Fig. 2, the SOA from *m*-xylene-OH experiments can be obviously observed under both two RH conditions. The intensities of all functional groups from the low RH experiment are much higher than those from the high RH experiment, which is consistent with the reduced SOA yields under elevated RH conditions.

The assignment and the intensity of the FTIR absorption frequencies at low (Exp. 2) and high (Exp. 6) RHs is summarized in Table 2. The broad absorption at 3600-2400 cm⁻¹ is O-H stretching vibration in phenol, hydroxyl and carboxyl groups (Stevenson and Goh, 1971; Santos and Duarte, 1998; Duarte et al., 2005). The band at 3000 cm⁻¹ is C-H stretching vibration (Stevenson and Goh, 1971; Santos and Duarte, 1998; Duarte et al., 2005). The sharp absorption at 1720 cm⁻¹ is the C=O stretching vibration in carboxylic acids, formate esters, aldehydes and ketones (Stevenson and Goh, 1971; Santos and Duarte, 1998; Duarte et al., 2005). The absorptions at 1605 cm⁻¹ match C-C stretching of aromatic rings and the C=O stretching of conjugated carbonyl groups. The absorptions at 1415 cm⁻¹ match the deformation of CO-H, phenolic O-H and C-O (Cory and Dillner, 2008; Ofner et al., 2011). The absorptions at 1180 cm⁻¹ match the C-O-C stretching of polymers, C-O and OH of COOH groups (Jang and Kamens, 2001; Jang et al., 2002; Duarte et al., 2005). The absorptions at 1080 cm⁻¹ match the C-C-OH stretching of alcohols (Jang and Kamens, 2001; Jang et al., 2002).

The absorption intensity at ~3200 cm⁻¹ that is identified as the hydroxyl group is used to be a representative for reflection of the SOA formation. As well, Table 2 gives the ratio of intensities at high RH (Exp. 6) to those at low RH (Exp. 2) to compare the difference of relative intensities of functional groups. The intensities of functional groups are obviously suppressed at high RH, but the extents of the suppression for different functional groups are basically divided into two types. The ratios of O-H, C-H, C=O and C-C-OH groups are 0.29 to 0.34, which is close to the ratio of SOA mass at high RH to that at low RH collected on the ZnSe disk, whereas the ratios of CO-H, C-O-C, C-O-H in COOH are above 0.48. The relative intensity of the C-O-C group is significantly higher than the C=O group, which can be explained by more oligomerization with the formation of C-O-C than other reactions at high RH. Nevertheless, the FTIR results cannot provide further information to well explain the differences of SOA yields between low and high RH, which will be further discussed in terms of mass spectra of SOA in the next section.

3.3 RH effects on mass spectra of SOA

We selected the sample mass spectra whose intensities are larger than 10^5 under the low RH condition and corresponding mass spectra under the high RH condition, followed by the blank mass spectra deduction. The blank-deducting mass spectra of SOA formed from *m*-xylene-OH photooxidation under low and high RH conditions in both positive and negative ion modes are presented in Fig. 3, which is plotted as a function of the mass-to-charge ratio. It should be noted that the Y-axis scales for low and high RH are largely different, 10^6 at low RH and 10^5 at high RH. As shown in Fig. 3, a visible decrease in the overall peak intensities for both positive and negative ion modes can be obviously observed as the RH elevates, which is consistent with the result that the SOA mass concentration is lower at high RH. In addition, it is obvious that the number of peaks is less under the high RH condition. As shown in Fig. 3, where the *m/z* values of SOA samples are close for both low and high conditions, the absolute and relative intensities of the peaks are much different, indicating that RH significantly affects the concentration of SOA components.

Table 3 lists the peaks whose intensities are larger than 10^6 of low RH samples and the structure can be proposed according to the gas-phase chemical mechanism of *m*-xylene-OH photooxidation included in MCM and the fragments from MS/MS analysed with Mass Frontier. In the positive ion mode, an $[M+H]^+$ ion of *m/z* = 137.05962 at low RH and 137.05931 at high RH is assigned as a molecular ion formula of $C_8H_9O_2^+$ that has a mass difference of $\Delta = 0.6$ and 1.0 mDa for low and high RH, respectively. The structure of identified compound $C_8H_8O_2$ is proposed to be 2,6-dimethyl-1,4-benzoquinone, the fragments of which from MS/MS match those from simulation of the Mass Frontier program. This compound was also identified and quantified in a previous study on SOA compositions from *m*-xylene- NO_x irradiation using the method of GC-MS analysis with authentic standards (Forstner et al., 1997). Thus, 2,6-dimethyl-1,4-benzoquinone was the SOA component partitioning into particle phase from the gas phase. The measured ion of *m/z* = 155.07013 at low RH and 155.06985 at high RH is assigned as a molecular ion formula of $C_8H_{11}O_3^+$ that has $\Delta = 1.2$ and 1.5 mDa, and its structure is proposed to be O=CC1(C)OC1C=CC(=O)C, an oxidized unsaturated epoxide. The measured ion of *m/z* = 171.06509 at low RH and 171.06488 at high RH is assigned as a molecular ion formula of $C_8H_{11}O_4^+$ that has $\Delta = 1.2$ and 1.4 mDa, the structure of which is proposed to be a bicyclic peroxide. The measured ion of *m/z* = 187.06003 at low RH and 187.05678 at high RH is assigned as a molecular ion formula of $C_8H_{11}O_5^+$ that has $\Delta = 1.2$ and 4.4 mDa, whose structure is proposed to be O=CC1(C)OC1C(O)C(=O)C(=O)C. All these SOA components are suppressed to almost disappear at high RH, except for 2,6-dimethyl-1,4-benzoquinone.

For rough quantification of the RH effect, the peaks in Figure 3 were assigned with the number of carbon atoms. The intensities of the peaks with the same number of carbon atoms (*nC*) are summed, which are presented in Figure 4. It should be noted that the Y-axis scales at low and high RHs are largely different, with a label step of 4.0×10^6 at low RH and 4.0×10^5 at high RH in the positive ion mode, 5.0×10^6 at low RH and 1.0×10^5 at high RH in the negative ion mode. The compounds with *nC* > 8, larger number of carbon atoms than *m*-xylene, are proposed to be oligomers that account for a large mass fraction of SOA due to their large molecular weights and lower volatilities, though their peak intensities are lower. As a

result, the processes for formation of such compounds play an important role in the formation of SOA. It can be obviously observed that the peak intensities are much lower at high RH in the negative ion mode than that in the positive mode, indicating that the decrease of the compounds obtained in the negative ion mode account for a larger decrease at high RH.

3.4 Proposed mechanism of RH effects on SOA formation

5 The large difference of SOA yields and composition between low and high RHs is proposed that water is directly involved in the chemical mechanism and further affects the SOA growth. In the particle-phase accretion equilibrium reactions, where water is involved as a by-product, the elevated RH alters the equilibrium of reaction by moving toward reducing the fraction of oligomers with low volatility and increasing the fraction of monomers (Nguyen et al., 2011; Hinks et al., 2018). In this study and the previous study on toluene SOA formation, C_2H_2O was one of the most frequent mass difference at low and
10 high RHs, but the peak intensities of its related compounds were much lower under elevated RH conditions (Hinks et al., 2018). C_2H_2O was proposed to be from the oligomerization reaction of glycolaldehyde ($C_2H_4O_2$), which can react with carbonyl compounds by aldol condensation reactions with water as the by-product. This chemistry may dominantly affect the negative RH effect on the whole process of SOA formation.

Moreover, there may exist other processes that enlarge the difference of SOA formation under various RH conditions.
15 Before we discuss the possible processes, the reaction pathway between *m*-xylene and OH radicals need to go through first. Reactions between *m*-xylene (C_8H_{10}) and OH radicals have two pathways, the H-abstraction from the methyl group and OH-addition to the aromatic ring, which generates products such as methylbenzaldehyde (C_8H_8O) and methylbenzyl alcohol ($C_8H_{10}O$), as shown in Scheme 1. OH-addition is the dominant pathway, as the branching ratio of H-abstraction only accounts for 4% based on MCM. OH-addition to the aromatic ring is followed by O_2 -adduct and isomerization to form a
20 carbon-centered radical, which can form a dimethylphenol ($C_8H_{10}O$) or is adducted by an O_2 molecule forming a bicyclic peroxy radical (BPR, $C_8H_{11}O_5$) (Calvert et al., 2002; Birdsall et al., 2010; Wu et al., 2014). The BPR reacts with other RO_2 radicals or HO_2 forming the bicyclic oxy radical ($C_8H_{11}O_4$). This RO radical can get further reaction and finally form carbonylic products, such as (methyl) glyoxal and other SOA precursors (Jenkin et al., 2003; Hallquist et al., 2009; Carlton et al., 2010; Carter and Heo, 2013), or react with HO_2 radicals forming bicyclic hydroxyhydroperoxides ($ROOH$, $C_8H_{12}O_5$),
25 or react with other RO_2 radicals forming ROH ($C_8H_{12}O_4$) and $R-HO$ ($C_8H_{10}O_4$). The self- and cross-reactions of RO_2 radicals also form $ROOR$ ($C_{16}H_{22}O_{10}$) or $ROOR'$ that is the accretion products (Berndt et al., 2018; Molteni et al., 2018). The further O_2 -adduct of BPR can form a highly-oxygenated RO_2 radicals and further get reacted and finally form highly oxygenated organic molecules (HOMs) (Types 1 and 2 in Scheme 1) (Wang et al., 2017; Crouse et al., 2013; Ehn et al., 2014; Jokinen et al., 2015; Berndt et al., 2016). Dimethylphenol ($C_8H_{10}O$) as well as other products from termination reaction with benzene
30 ring or double bond can react with OH radicals and get further reacted to form HOMs as well.

Most of HOMs can fall into extremely low or low volatility organic compounds ((E)LVOCs) and a small number of HOMs are semi-volatility organic compounds (SVOC) (Bianchi et al., 2019). ELVOCs can condense onto particles but SVOCs exist in significant fractions in both the condensed and gas phases at equilibrium. As SMPS measured, at the end of the

experiment the number concentrations (not corrected) of Exp. 1 (low RH) and Exp. 7 (high RH) were 1.9×10^3 and 5.8×10^2 particles cm^{-3} , with a factor of 3; while the mass concentrations (not corrected) of Exp. 1 (low RH) and Exp. 7 (high RH) were 116.9 and 8.7 $\mu\text{g m}^{-3}$, with a factor of 13. This indicates that the size of particles at low RH are higher than that at high RH. The O:C ratios in positive and negative ion modes under low and high RH conditions were roughly calculated using the carbon and oxygen atom numbers multiplied by the relative intensities obtained by HRMS. The O:C ratio in the positive ion mode was close to each other, 0.56 and 0.58 at low and high RHs, respectively; while the O:C ratio in the negative ion mode was differential, 0.66 and 0.77 at low and high RHs, respectively. Based on the gas to particle partitioning rule, the more volatile compounds in the gas phase can condense to the particles with larger size (Li et al., 2018). It can be deduced that the particles with larger size at the reduced RH result in more SVOC in the gas phase to condense, leading to the difference of SOA mass at various RHs. As shown in Fig. 5, more compounds with less nC ($\text{nC} < 8$) are present under the low RH experiment, also indicating that more SVOCs in the gas phase condense onto the particles.

The higher O:C ratio in the negative ion mode demonstrates that the compounds in the negative ion mode are much more oxygenated than those in the positive ion mode. As shown in Fig. 5, the peak intensities at high RH are much lower in the negative ion mode than in the positive mode, indicating that the decrease of the more oxygenated compounds accounts for the larger fraction at high RH. These high O:C ratios cannot be explained by any of the formerly known oxidation pathways, except that the formation of HOMs from RO_2 autoxidation is taken into consideration (Crounse et al., 2013; Barsanti et al., 2017). To our knowledge, RH does not directly impact the formation of HOMs (Li et al., 2019). It is possible that HOMs undergo further particle-phase reactions as it has been suggested in a few studies (Bianchi et al., 2019) which may be influenced by RH, but this process need to be further investigated in the future studies. Moreover, the wall process of the reactor enlarges the difference of SOA mass between low and high RH. The wall loss of some chemical species is faster at high RH, which leads to the reduction of SOA yield.

4. Conclusion and atmospheric implication

The current study investigates the effect of RH on SOA formation from the oxidation of *m*-xylene under low NO_x conditions in the absence of seed particles. The elevated RH can significantly obstruct the SOA formation from the *m*-xylene-OH system, so that the SOA yield decrease from 14.6% at low RH to 0.8% at high RH, with a significant discrepancy of higher than one order of magnitude. The FTIR analysis shows that the proportion of oligomers with C-O-C groups from carbonyl compounds in SOA at high RH is higher than that at low RH, but the negative RH effect on SOA formation cannot be well explained as the FTIR results cannot provide further information. From the analysis of the HRMS spectra, it is found that $\text{C}_2\text{H}_2\text{O}$ is one of the most common mass difference at low and high RHs, that the compounds with lower carbon number in the formula at low RH account for a larger proportion than those at high RH, and that the compounds at high RH have higher O:C ratios than those at low RH. The HRMS results suggest that the RH may suppress the oligomerization where water is involved as a by-product and may influence the further particle-phase reaction of high oxygenated organic molecules (HOMs)

formed in the gas phase. In addition to the chemical processes, the negative RH effect on SOA formation is enlarged based on the gas to particle partitioning rule. Together with the previous study on toluene SOA, it is conceivable that the effect of RH on SOA yield is a common feature of SOA formation from monocyclic aromatics oxidation under low NO_x conditions and using H₂O₂ as the OH radical source. Our results obviously indicate that the production of SOA from aromatics in low-NO_x environments can be strongly modulated by the ambient RH. Our study highlights the role of water in the SOA formation, which is particularly related to chemical mechanisms used to explain observed air quality and to predict chemistry in air quality models and climate models. The clear pathway of the influence of H₂O on the particle phase reaction of HOMs formed in the gas phase needs to be further studied in the future.

Author contribution

Qun Zhang and Yongfu Xu designed the research. Qun Zhang carried out the experiments and analyzed the data. Long Jia provided valuable advices on the experiment operations. Yongfu Xu and Long Jia provided advices on the analysis of results. Qun Zhang prepared the manuscript with contributions from all co-authors.

Acknowledgments

This work was supported by the National Key R&D Program of China (2017YFC0210005) and National Natural Science Foundation of China (No. 41375129).

References

- Barsanti, K. C., Kroll, J. H., and Thornton, J. A.: Formation of low-volatility organic compounds in the atmosphere: Recent advancements and insights, *J. Phys. Chem. Lett.*, 8, 1503-1511, 10.1021/acs.jpcclett.6b02969, 2017.
- Berndt, T., Richters, S., Jokinen, T., Hyttinen, N., Kurten, T., Otkjaer, R. V., Kjaergaard, H. G., Stratmann, F., Herrmann, H., Sipila, M., Kulmala, M., and Ehn, M.: Hydroxyl radical-induced formation of highly oxidized organic compounds, *Nat. Commun.*, 7, 13677, 10.1038/ncomms13677, 2016.
- Berndt, T., Scholz, W., Mentler, B., Fischer, L., Herrmann, H., Kulmala, M., and Hansel, A.: Accretion product formation from self- and cross-reactions of RO₂ radicals in the atmosphere, *Angew. Chem. Int. Ed.*, 57, 3820-3824, 10.1002/anie.201710989, 2018.
- Betterton, E. A., and Hoffmann, M. R.: Henry's law constants of some environmentally important aldehydes, *Environ. Sci. Technol.*, 22, 1415-1418, 10.1021/es00177a004, 1988.
- Bianchi, F., Kurten, T., Riva, M., Mohr, C., Rissanen, M. P., Roldin, P., Berndt, T., Crouse, J. D., Wennberg, P. O., Mentel, T. F., Wildt, J., Junninen, H., Jokinen, T., Kulmala, M., Worsnop, D. R., Thornton, J. A., Donahue, N., Kjaergaard, H. G.,

- and Ehn, M.: Highly oxygenated organic molecules (HOM) from gas-phase autoxidation involving peroxy radicals: a key contributor to atmospheric aerosol, *Chem. Rev.*, 119, 3472-3509, 10.1021/acs.chemrev.8b00395, 2019.
- Birdsall, A. W., Andreoni, J. F., and Elrod, M. J.: Investigation of the role of bicyclic peroxy radicals in the oxidation mechanism of toluene, *J. Phys. Chem. A*, 114, 10655-10663, 10.1021/jp105467e, 2010.
- 5 Bloss, C., Wagner, V., Jenkin, M. E., Volkamer, R., Bloss, W. J., Lee, J. D., Heard, D. E., Wirtz, K., Martin-Reviejo, M., Rea, G., Wenger, J. C., and Pilling, M. J.: Development of a detailed chemical mechanism (MCMv3.1) for the atmospheric oxidation of aromatic hydrocarbons, *Atmos. Chem. Phys.*, 5, 641-664, 10.5194/acp-5-641-2005, 2005.
- Calvert, J. G., Atkinson, R., Becker, K. H., Kamens, R. M., Seinfeld, J. H., Wallington, T. H., and Yarwood, G.: *The mechanisms of atmospheric oxidation of the aromatic hydrocarbons*, Oxford University Press, 2002.
- 10 Cao, G., and Jang, M.: An SOA model for toluene oxidation in the presence of inorganic aerosols, *Environ. Sci. Technol.*, 44, 727-733, 10.1021/es901682r, 2010.
- Carlton, A. G., Bhave, P. V., Napelenok, S. L., Edney, E. O., Golam, S., Pinder, R. W., Pouliot, G. A., and Marc, H.: Model representation of secondary organic aerosol in CMAQv4.7, *Environ. Sci. Technol.*, 44, 8553-8560, 10.1021/es100636q, 2010.
- 15 Carter, W. P. L., and Heo, G.: Development of revised SAPRC aromatics mechanisms, *Atmos. Environ.*, 77, 404-414, 10.1016/j.atmosenv.2013.05.021, 2013.
- Coury, C., and Dillner, A. M.: A method to quantify organic functional groups and inorganic compounds in ambient aerosols using attenuated total reflectance FTIR spectroscopy and multivariate chemometric techniques, *Atmos. Environ.*, 42, 5923-5932, 10.1016/j.atmosenv.2008.03.026, 2008.
- 20 Crounse, J. D., Nielsen, L. B., Jørgensen, S., Kjaergaard, H. G., and Wennberg, P. O.: Autoxidation of organic compounds in the atmosphere, *J. Phys. Chem. Lett.*, 4, 3513-3520, 10.1021/jz4019207, 2013.
- Czoschke, N. M., Jang, M., and Kamens, R. M.: Effect of acidic seed on biogenic secondary organic aerosol growth, *Atmos. Environ.*, 37, 4287-4299, 10.1016/s1352-2310(03)00511-9, 2003.
- Ding, X., Wang, X.-M., Gao, B., Fu, X.-X., He, Q.-F., Zhao, X.-Y., Yu, J.-Z., and Zheng, M.: Tracer-based estimation of secondary organic carbon in the Pearl River Delta, south China, *J. Geophys. Res.*, 117, D05313, 10.1029/2011jd016596, 2012.
- 25 Duarte, R. M. B. O., Pio, C. A., and Duarte, A. C.: Spectroscopic study of the water-soluble organic matter isolated from atmospheric aerosols collected under different atmospheric conditions, *Analytica Chimica Acta*, 530, 7-14, 10.1016/j.aca.2004.08.049, 2005.
- 30 Durand, T., Bau, S., Morele, Y., Matera, V., Bémer, D., and Rousset, D.: Quantification of low pressure impactor wall deposits during zinc nanoparticle sampling, *Aerosol Air Qual. Res.*, 14, 1812-1821, 10.4209/aaqr.2013.10.0304, 2014.
- Ehn, M., Thornton, J. A., Kleist, E., Sipilä, M., Junninen, H., Pullinen, I., Springer, M., Rubach, F., Tillmann, R., and Lee, B.: A large source of low-volatility secondary organic aerosol, *Nature*, 506, 476-479, 10.1038/nature13032, 2014.

- Engelhart, G. J., Hildebrandt, L., Kostenidou, E., Mihalopoulos, N., Donahue, N. M., and Pandis, S. N.: Water content of aged aerosol, *Atmos. Chem. Phys.*, 11, 911-920, 10.5194/acp-11-911-2011, 2011.
- Faust, J. A., Wong, J. P. S., Lee, A. K. Y., and Abbatt, J. P. D.: Role of aerosol liquid water in secondary organic aerosol formation from volatile organic compounds, *Environ. Sci. Technol.*, 51, 1405-1413, 10.1021/acs.est.6b04700, 2017.
- 5 Finlayson-Pitts, B. J., and Pitts Jr., J. N.: Chapter 6-Rates and mechanisms of gas-phase reactions in irradiated organic-NO_x-air mixtures, in: *Chemistry of the Upper and Lower Atmosphere*, Academic Press, San Diego, 179-263, 2000.
- Forstner, H. J. L., Flagan, R. C., and Seinfeld, J. H.: Secondary organic aerosol from the photooxidation of aromatic hydrocarbons: Molecular composition, *Environ. Sci. Technol.*, 31, 1345-1358, 10.1021/es9605376, 1997.
- Ge, S., Xu, Y., and Jia, L.: Secondary organic aerosol formation from ethyne in the presence of NaCl in a smog chamber, 10 *Environ. Chem.*, 13, 699-710, 10.1071/en15155, 2016.
- Ge, S., Xu, Y., and Jia, L.: Effects of inorganic seeds on secondary organic aerosol formation from photochemical oxidation of acetone in a chamber, *Atmos. Environ.*, 170, 205-215, 10.1016/j.atmosenv.2017.09.036, 2017a.
- Ge, S., Xu, Y., and Jia, L.: Secondary organic aerosol formation from propylene irradiations in a chamber study, *Atmos. Environ.*, 157, 146-155, 10.1016/j.atmosenv.2017.03.019, 2017b.
- 15 Ge, S., Xu, Y., and Jia, L.: Secondary organic aerosol formation from ethylene ozonolysis in the presence of sodium chloride, *J. Aerosol Sci.*, 106, 120-131, 10.1016/j.jaerosci.2017.01.009, 2017c.
- Hallquist, M., Wenger, J. C., Baltensperger, U., Rudich, Y., Simpson, D., Claeys, M., Dommen, J., Donahue, N. M., George, C., Goldstein, A. H., Hamilton, J. F., Herrmann, H., Hoffmann, T., Iinuma, Y., Jang, M., Jenkin, M. E., Jimenez, J. L., Kiendler-Scharr, A., Maenhaut, W., McFiggans, G., Mentel, T. F., Monod, A., Prévôt, A. S. H., Seinfeld, J. H., Surratt, J. D., 20 Szmigielski, R., and Wildt, J.: The formation, properties and impact of secondary organic aerosol: current and emerging issues, *Atmos. Chem. Phys.*, 9, 5155-5236, 10.5194/acp-9-5155-2009, 2009.
- Hansen, J. E., and Sato, M.: Trends of measured climate forcing agents, *Proc. Natl. Acad. Sci. U. S. A.*, 98, 14778-14783, 10.1073/pnas.261553698, 2001.
- Healy, R. M., Temime, B., Kuprovskite, K., and Wenger, J. C.: Effect of relative humidity on gas/particle partitioning and 25 aerosol mass yield in the photooxidation of *p*-xylene, *Environ. Sci. Technol.*, 43, 1884-1889, 10.1021/es802404z, 2009.
- Hinks, M. L., Montoya-Aguilera, J., Ellison, L., Lin, P., Laskin, A., Laskin, J., Shiraiwa, M., Dabdub, D., and Nizkorodov, S. A.: Effect of relative humidity on the composition of secondary organic aerosol from the oxidation of toluene, *Atmos. Chem. Phys.*, 18, 1643-1652, 10.5194/acp-18-1643-2018, 2018.
- Huang, R. J., Zhang, Y., Bozzetti, C., Ho, K. F., Cao, J. J., Han, Y., Daellenbach, K. R., Slowik, J. G., Platt, S. M., Canonaco, 30 F., Zotter, P., Wolf, R., Pieber, S. M., Bruns, E. A., Crippa, M., Ciarelli, G., Piazzalunga, A., Schwikowski, M., Abbaszade, G., Schnelle-Kreis, J., Zimmermann, R., An, Z., Szidat, S., Baltensperger, U., El Haddad, I., and Prevot, A. S.: High secondary aerosol contribution to particulate pollution during haze events in China, *Nature*, 514, 218-222, 10.1038/nature13774, 2014.

- Ip, H. S. S., Huang, X. H. H., and Yu, J. Z.: Effective Henry's law constants of glyoxal, glyoxylic acid, and glycolic acid, *Geophys. Res. Lett.*, 36, L01802, 10.1029/2008gl036212, 2009.
- Jacobson, M. C., Hansson, H. C., Noone, K. J., and Charlson, R. J.: Organic atmospheric aerosols: Review and state of the science, *Rev. Geophys.*, 38, 267-294, 10.1029/1998rg000045, 2000.
- 5 Jang, M., Czoschke, N. M., Lee, S., and Kamens, R. M.: Heterogeneous atmospheric aerosol production by acid-catalyzed particle-phase reactions, *Science*, 298, 814-817, 10.1126/science.1075798, 2002.
- Jang, M. S., and Kamens, R. M.: Characterization of secondary aerosol from the photooxidation of toluene in the presence of NO_x and 1-propene, *Environ. Sci. Technol.*, 35, 3626-3639, 10.1021/es010676+, 2001.
- Jenkin, M. E., Saunders, S. M., Wagner, V., and Pilling, M. J.: Protocol for the development of the Master Chemical
10 Mechanism, MCM v3 (Part B): tropospheric degradation of aromatic volatile organic compounds, *Atmos. Chem. Phys.*, 3, 181-193, 10.5194/acp-3-181-2003, 2003.
- Jia, L., and Xu, Y.: Effects of relative humidity on ozone and secondary organic aerosol formation from the photooxidation of benzene and ethylbenzene, *Aerosol Sci. Technol.*, 48, 1-12, 10.1080/02786826.2013.847269, 2014.
- Jia, L., and Xu, Y.: Ozone and secondary organic aerosol formation from Ethylene-NO_x -NaCl irradiations under different
15 relative humidity conditions, *J. Atmos. Chem.*, 73, 81-100, 10.1007/s10874-015-9317-1, 2016.
- Jia, L., and Xu, Y.: Different roles of water in secondary organic aerosol formation from toluene and isoprene, *Atmos. Chem. Phys.*, 18, 8137-8154, 10.5194/acp-18-8137-2018, 2018.
- Jokinen, T., Sipilä, M., Richters, S., Kerminen, V. M., Paasonen, P., Stratmann, F., Worsnop, D., Kulmala, M., Ehn, M., and Herrmann, H.: Rapid autoxidation forms highly oxidized RO₂ radicals in the atmosphere, *Angew. Chem. Int. Ed.*, 53, 14596-
20 14600, 10.1002/anie.201408566, 2015.
- Kamens, R. M., Zhang, H., Chen, E. H., Zhou, Y., Parikh, H. M., Wilson, R. L., Galloway, K. E., and Rosen, E. P.: Secondary organic aerosol formation from toluene in an atmospheric hydrocarbon mixture: Water and particle seed effects, *Atmos. Environ.*, 45, 2324-2334, 10.1016/j.atmosenv.2010.11.007, 2011.
- Kanakidou, M., Seinfeld, J. H., Pandis, S. N., Barnes, I., Dentener, F. J., Facchini, M. C., Dingenen, R. V., Ervens, B., Nenes,
25 A., Nielsen, C. J., Swietlicki, E., Putaud, J. P., Balkanski, Y., Fuzzi, S., Horth, J., Moortgat, G. K., Winterhalter, R., Myhre, C. E. L., Tsigaridis, K., Vignati, E., Stephanou, E. G., and Wilson, J.: Organic aerosol and global climate modelling: a review, *Atmos. Chem. Phys.*, 5, 1053-1123, 10.5194/acp-5-1053-2005, 2005.
- Khoder, M. I.: Ambient levels of volatile organic compounds in the atmosphere of Greater Cairo, *Atmos. Environ.*, 41, 554-566, 10.1016/j.atmosenv.2006.08.051, 2007.
- 30 Kidd, C., Perraud, V., Wingen, L. M., and Finlayson-Pitts, B. J.: Integrating phase and composition of secondary organic aerosol from the ozonolysis of α -pinene, *Proc. Natl. Acad. Sci. U. S. A.*, 111, 7552-7557, 10.1073/pnas.1322558111, 2014.
- Li, K., Li, J., Wang, W., Li, J., Peng, C., Wang, D., and Ge, M.: Effects of gas-particle partitioning on refractive index and chemical composition of *m*-xylene secondary organic aerosol, *J. Phys. Chem. A*, 122, 3250-3260, 10.1021/acs.jpca.7b12792, 2018.

- Li, X., Chee, S., Hao, J., Abbatt, J. P. D., Jiang, J., and Smith, J. N.: Relative humidity effect on the formation of highly oxidized molecules and new particles during monoterpene oxidation, *Atmos. Chem. Phys.*, 19, 1555-1570, 10.5194/acp-19-1555-2019, 2019.
- Liu, T., Huang, D., Li, Z., Liu, Q., Chan, M., and Chan, C. K.: Comparison of secondary organic aerosol formation from toluene on initially wet and dry ammonium sulfate particles at moderate relative humidity, *Atmos. Chem. Phys.*, 18, 5677-5689, 10.5194/acp-18-5677-2018, 2018.
- Liu, Y., Wu, Z., and Hu, M.: Advances in the phase state of secondary organic aerosol (in Chinese), *China Environ. Sci.*, 37, 1637-1645, 2017.
- Loza, C. L., Chhabra, P. S., Yee, L. D., Craven, J. S., Flagan, R. C., and Seinfeld, J. H.: Chemical aging of *m*-xylene secondary organic aerosol: laboratory chamber study, *Atmos. Chem. Phys.*, 12, 151-167, 10.5194/acp-12-151-2012, 2012.
- Matsunaga, A., and Ziemann, P. J.: Gas-wall partitioning of organic compounds in a Teflon film chamber and potential effects on reaction product and aerosol yield measurements, *Aerosol Sci. Technol.*, 44, 881-892, 10.1080/02786826.2010.501044, 2010.
- Molteni, U., Bianchi, F., Klein, F., El Haddad, I., Frege, C., Rossi, M. J., Dommen, J., and Baltensperger, U.: Formation of highly oxygenated organic molecules from aromatic compounds, *Atmos. Chem. Phys.*, 18, 1909-1921, 10.5194/acp-18-1909-2018, 2018.
- Nah, T., McVay, R. C., Zhang, X., Boyd, C. M., Seinfeld, J. H., and Ng, N. L.: Influence of seed aerosol surface area and oxidation rate on vapor wall deposition and SOA mass yields: a case study with α -pinene ozonolysis, *Atmos. Chem. Phys.*, 16, 9361-9379, 10.5194/acp-16-9361-2016, 2016.
- Nah, T., McVay, R. C., Pierce, J. R., Seinfeld, J. H., and Ng, N. L.: Constraining uncertainties in particle-wall deposition correction during SOA formation in chamber experiments, *Atmos. Chem. Phys.*, 17, 2297-2310, 10.5194/acp-17-2297-2017, 2017.
- Ng, N. L., Kroll, J. H., Chan, A. W. H., Chhabra, P. S., Flagan, R. C., and Seinfeld, J. H.: Secondary organic aerosol formation from *m*-xylene, toluene, and benzene, *Atmos. Chem. Phys.*, 7, 3909-3922, 10.5194/acp-7-3909-2007, 2007.
- Nguyen, T. B., Roach, P. J., Laskin, J., Laskin, A., and Nizkorodov, S. A.: Effect of humidity on the composition of isoprene photooxidation secondary organic aerosol, *Atmos. Chem. Phys.*, 11, 6931-6944, 10.5194/acp-11-6931-2011, 2011.
- Odum, J. R., Jungkamp, T. P., Griffin, R. J., Flagan, R. C., and Seinfeld, J. H.: The atmospheric aerosol-forming potential of whole gasoline vapor, *Science*, 276, 96-99, 10.1126/science.276.5309.96, 1997.
- Offenberg, J. H., Lewis, C. W., Lewandowski, M., Jaoui, M., Kleindienst, T. E., and Edney, E. O.: Contributions of toluene and α -pinene to SOA formed in an irradiated toluene/ α -pinene/ NO_x /air mixture: comparison of results using ^{14}C content and SOA organic tracer methods, *Environ. Sci. Technol.*, 41, 3972-3976, 10.1021/es070089+, 2007.
- Ofner, J., Kruger, H.-U., H., G., Schmitt-Kopplin, P., Whitmore, K., and Zetzsch, C.: Physico-chemical characterization of SOA derived from catechol and guaiacol-a model substance for the aromatic fraction of atmospheric HULIS, *Atmos. Chem. Phys.*, 11, 1-15, 10.5194/acp-11-1-2011, 2011.

- Poulain, L., Katrib, Y., Isikli, E., Liu, Y., Wortham, H., Mirabel, P., Le Calve, S., and Monod, A.: In-cloud multiphase behaviour of acetone in the troposphere: gas uptake, Henry's law equilibrium and aqueous phase photooxidation, *Chemosphere*, 81, 312-320, 10.1016/j.chemosphere.2010.07.032, 2010.
- 5 Qi, L., Nakao, S., Tang, P., and Cocker, D. R., III: Temperature effect on physical and chemical properties of secondary organic aerosol from *m*-xylene photooxidation, *Atmos. Chem. Phys.*, 10, 3847-3854, 10.5194/acp-10-3847-2010, 2010.
- Santos, E. B. H., and Duarte, A. C.: The influence of pulp and paper mill effluents on the composition of the humic fraction of aquatic organic matter, *Wat. Res.*, 32, 597-608, 10.1016/S0043-1354(97)00301-1, 1998.
- Seinfeld, J. H., and Pandis, S. N.: *Atmospheric chemistry and physics: From air pollution to climate change*, 3rd ed., Wiley, Hoboken, 2016.
- 10 Song, C., Na, K., Warren, B., Malloy, Q., and Cocker, D. R., III: Secondary organic aerosol formation from *m*-xylene in the absence of NO_x, *Environ. Sci. Technol.*, 41, 7409-7416, 10.1021/es070429r, 2007.
- Spracklen, D. V., Jimenez, J. L., Carslaw, K. S., Worsnop, D. R., Evans, M. J., Mann, G. W., Zhang, Q., Canagaratna, M. R., Allan, J., Coe, H., McFiggans, G., Rap, A., and Forster, P.: Aerosol mass spectrometer constraint on the global secondary organic aerosol budget, *Atmos. Chem. Phys.*, 11, 12109-12136, 10.5194/acp-11-12109-2011, 2011.
- 15 Stevenson, F. J., and Goh, K. M.: Infrared spectra of humic acids and related substances, *Geochim. Cosmochim. Acta*, 35, 471-483, 10.1016/0016-7037(71)90044-5, 1971.
- Tuet, W. Y., Chen, Y., Xu, L., Fok, S., Gao, D., Weber, R. J., and Ng, N. L.: Chemical oxidative potential of secondary organic aerosol (SOA) generated from the photooxidation of biogenic and anthropogenic volatile organic compounds, *Atmos. Chem. Phys.*, 17, 839-853, 10.5194/acp-17-839-2017, 2017.
- 20 Wang, S., Wu, R., Berndt, T., Ehn, M., and Wang, L.: Formation of Highly Oxidized Radicals and Multifunctional Products from the Atmospheric Oxidation of Alkylbenzenes, *Environ. Sci. Technol.*, 51, 8442-8449, 10.1021/acs.est.7b02374, 2017.
- Wang, Y., Luo, H., Jia, L., and Ge, S.: Effect of particle water on ozone and secondary organic aerosol formation from benzene-NO₂-NaCl irradiations, *Atmos. Environ.*, 140, 386-394, 10.1016/j.atmosenv.2016.06.022, 2016.
- Warren, B., Song, C., and Cocker, D. R., III: Light intensity and light source influence on secondary organic aerosol formation for the *m*-xylene/NO_x photooxidation system, *Environ. Sci. Technol.*, 42, 5461-5466, 10.1021/es702985n, 2008.
- 25 Wu, R., Pan, S., Li, Y., and Wang, L.: Atmospheric oxidation mechanism of toluene, *J. Phys. Chem. A*, 118, 4533-4547, 10.1021/jp500077f, 2014.
- Zhang, X., Cappa, C. D., Jathar, S. H., McVay, R. C., Ensberg, J. J., Kleeman, M. J., and Seinfeld, J. H.: Influence of vapor wall loss in laboratory chambers on yields of secondary organic aerosol, *Proc. Natl. Acad. Sci. U. S. A.*, 111, 5802-5807, 10.1073/pnas.1404727111, 2014.
- 30 Zhang, X., Schwantes, R. H., McVay, R. C., Lignell, H., Coggon, M. M., Flagan, R. C., and Seinfeld, J. H.: Vapor wall deposition in Teflon chambers, *Atmos. Chem. Phys.*, 15, 4197-4214, 10.5194/acp-15-4197-2015, 2015.

Zhang, X., Dalleska, N. F., Huang, D. D., Bates, K. H., Sorooshian, A., Flagan, R. C., and Seinfeld, J. H.: Time-resolved molecular characterization of organic aerosols by PILS + UPLC/ESI-Q-TOFMS, *Atmos. Environ.*, 130, 180-189, 10.1016/j.atmosenv.2015.08.049, 2016.

5 Zhao, Y., Saleh, R., Saliba, G., Presto, A. A., Gordon, T. D., Drozd, G. T., Goldstein, A. H., Donahue, N. M., and Robinson, A. L.: Reducing secondary organic aerosol formation from gasoline vehicle exhaust, *Proc. Natl. Acad. Sci. U. S. A.*, 114, 6984-6989, 10.1073/pnas.1620911114, 2017.

Zhou, Y., Zhang, H., Parikh, H. M., Chen, E. H., Rattanavaraha, W., Rosen, E. P., Wang, W., and Kamens, R. M.: Secondary organic aerosol formation from xylenes and mixtures of toluene and xylenes in an atmospheric urban hydrocarbon mixture: Water and particle seed effects (II), *Atmos. Environ.*, 45, 3882-3890, 10.1016/j.atmosenv.2010.12.048,
10 2011.

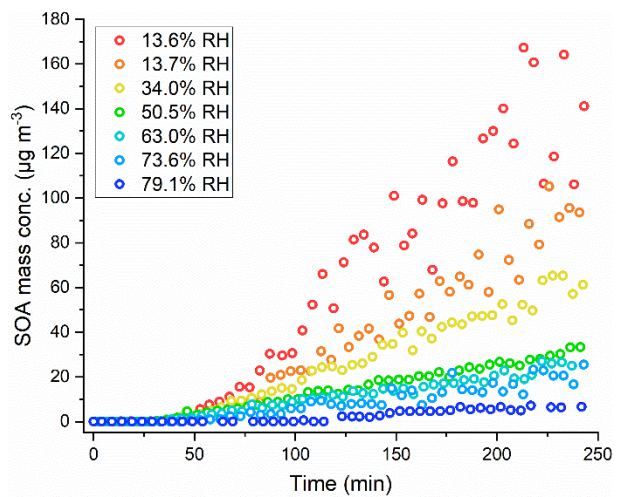


Figure 1. SOA mass concentrations as a function of irradiation time (corrected by particle wall loss).

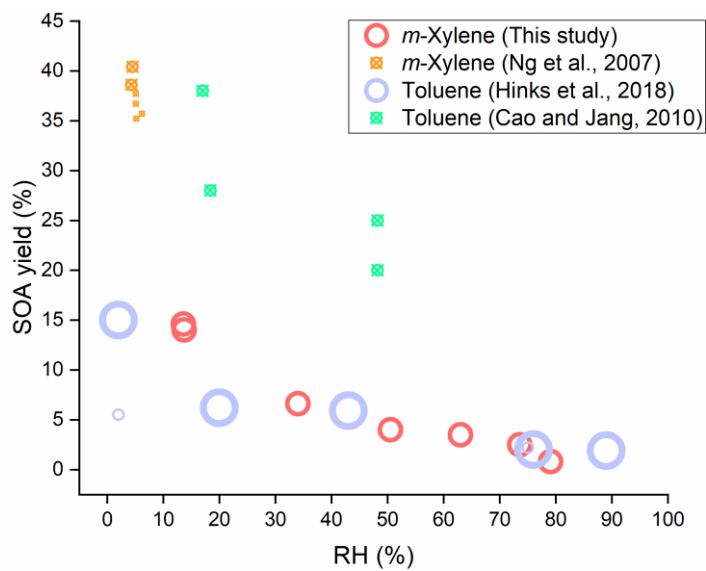


Figure 2. SOA yields as a function of RH for the different aromatic (toluene and *m*-xylene) oxidation under low NO_x conditions with the photolysis of H₂O₂ as the OH source. The hollow circles represent that no seed particles were introduced and the circles with a cross represent that seed particles were introduced. The size of markers indicates the magnitude of amount of reacted VOC.

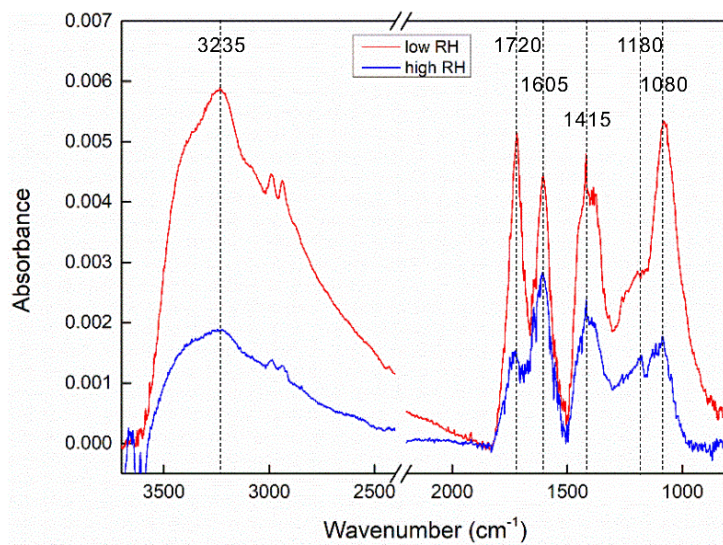
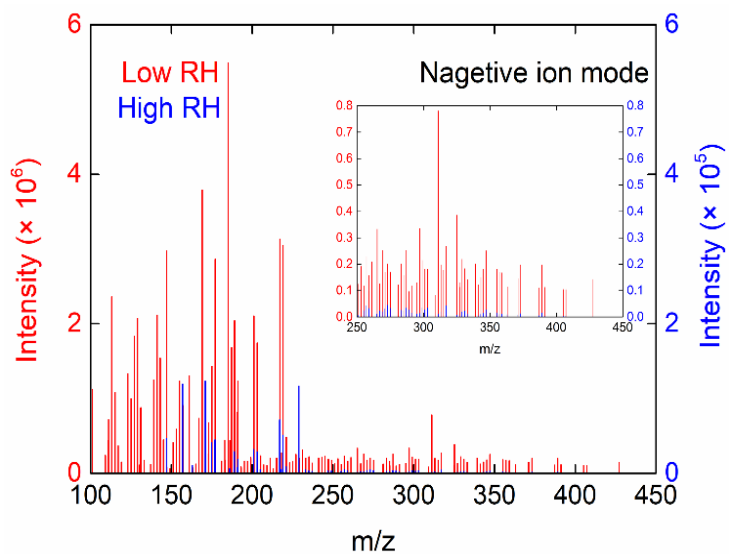
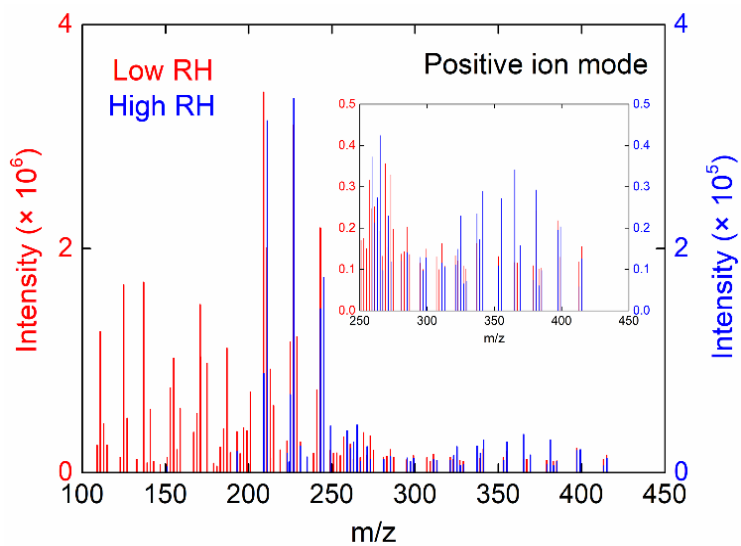
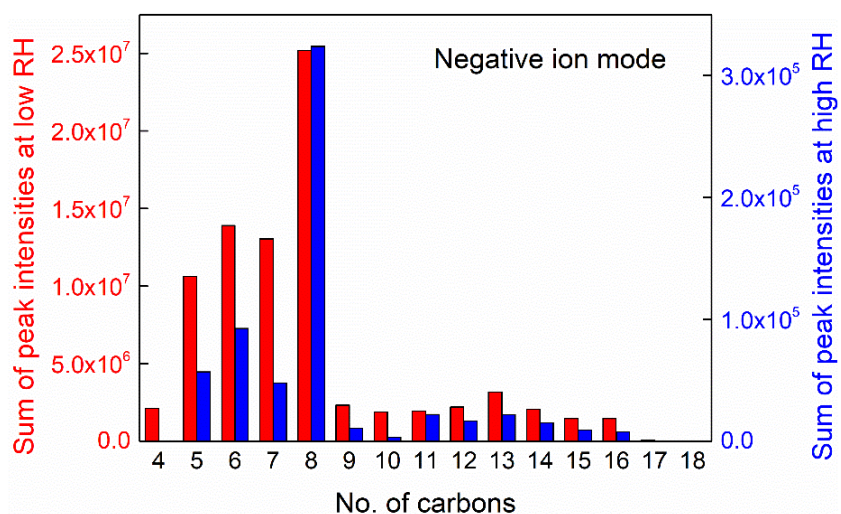
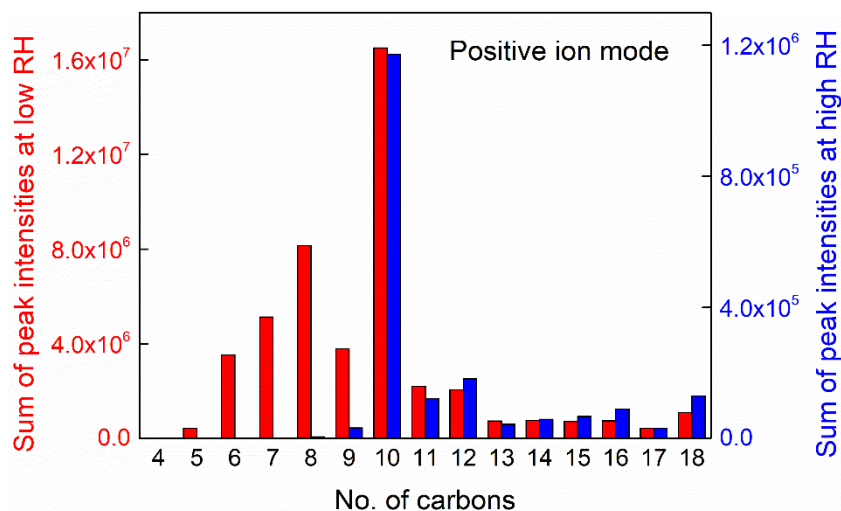


Figure 3. FTIR spectra of particles from photooxidation of *m*-xylene-OH experiments under low and high RH conditions.



5 **Figure 4.** Selected background-subtraction HESI-Q Exactive-Orbitrap MS results of SOA in both positive and negative ion modes from the photooxidation of *m*-xylene-OH under both low and high RH conditions (Note that the Y-axis scales for low and high RH are largely different, 10^6 at low RH and 10^5 at high RH).



5 **Figure 5.** Sum of peak intensities based on peaks selected in Figure 3 as a function of the number of carbon atoms under the positive ion mode and negative ion mode (Note that the Y-axis scale at low and high RH are largely different, with a label step of 4.0×10^6 at low RH and 4.0×10^5 at high RH in the positive ion mode, 5.0×10^6 at low RH and 1.0×10^5 at high RH in the negative ion mode).

Table 1. Experimental conditions and results at 4 h of experiments in *m*-xylene-H₂O₂ photooxidation system.

Exp. No.	[<i>m</i> -xylene] ₀ (μg m ⁻³)	[H ₂ O ₂] ₀ ^a (ppm)	RH (%)	T (°C)	[<i>m</i> -xylene] _{reacted} (μg m ⁻³)	[LWC] _{4h} ^b (μg m ⁻³)	[SOA] _{4h} ^b (μg m ⁻³)	SOA yield (%)
1	2287.9	20	13.6	25.9	1026.3	-	150.3 ± 15.0	14.6 ± 1.5
2	1855.5	20	13.7	25.3	682.0	-	95.5 ± 9.5	14.0 ± 1.4
3	2157.1	20	34.0	26.0	922.9	3.5 ± 0.3	61.1 ± 6.1	6.6 ± 0.7
4	2041.9	20	50.5	25.5	837.2	2.9 ± 0.3	33.3 ± 3.3	4.0 ± 0.4
5	2233.3	20	63.0	25.9	722.5	5.4 ± 0.5	25.0 ± 2.5	3.5 ± 0.3
6	2410.8	20	73.6	27.5	841.4	7.7 ± 0.8	21.0 ± 2.1	2.5 ± 0.2
7	2029.1	20	79.1	27.4	946.9	4.4 ± 0.4	7.5 ± 0.7	0.8 ± 0.1

^aCalculated using the density and mass concentration of injected H₂O₂ solution, and the volume of the reactor.

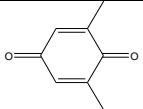
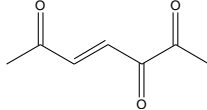
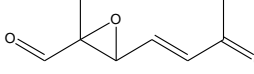
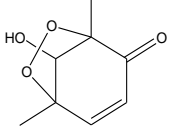
^bThe mass concentration at 4 h of reaction time with particle wall loss corrected.

Table 2. Absorbance positions of functional groups and the intensities at low (Exp. 2) and high (Exp. 6) RHs.

Absorption frequencies	Functionality	Intensity ($\times 10^{-3}$)		Ratio ^a
		low RH	high RH	
3235	O-H	5.9	1.9	0.32
3000	C-H	4.5	1.4	0.31
1720	C=O	5.1	1.5	0.29
1605	C-C of aromatic rings and conjugated C=O	4.4	2.8	0.64
1415	CO-H	4.8	2.4	0.50
1180	C-O-C, C-O and OH of COOH	2.9	1.4	0.48
1080	C-C-OH	5.3	1.8	0.34

^a Ratio of the intensity at high RH to that at low RH.

Table 3. Plausibility of different types of compounds with elemental formulae measured by HRMS in the positive ion mode.

Low RH			High RH			Ion formula	Proposed structure
Measured (m/z)	Intensity	Error (mDa)	Measured (m/z)	Intensity	Error (mDa)		
137.0596	1.7×10^6	0.6	137.0593	1.4×10^5	1.0	[C ₈ H ₉ O ₂] ⁺	
141.0545	5.6×10^6	1.3	141.0542	-	1.5	[C ₇ H ₉ O ₃] ⁺	
155.0701	1.0×10^6	1.2	155.0699	-	1.5	[C ₈ H ₁₁ O ₃] ⁺	
171.0651	1.0×10^6	1.2	171.0649	-	1.4	[C ₈ H ₁₁ O ₄] ⁺	
187.0600	1.1×10^6	1.2	187.0568	-	4.4	[C ₈ H ₁₁ O ₅] ⁺	